Large scale facies change in the middle Eocene South-Pyrenean foreland basin: The role of tectonics and prelude to Cenozoic ice-ages

Huyghe, Damien; Castelltort, Sébastien; Mouthereau, Frédéric; Serra-Kiel, Josep; Filleaudeau, Pierre-Yves; Emmanuel, Laurent; Berthier, Benoît; Renard, Maurice

How to cite

HUYGHE, Damien et al. Large scale facies change in the middle Eocene South-Pyrenean foreland basin: The role of tectonics and prelude to Cenozoic ice-ages. In: Sedimentary geology, 2012, vol. 253-254, p. 25–46. doi: 10.1016/j.sedgeo.2012.01.004

This publication URL: https://archive-ouverte.unige.ch/unige:20393
Publication DOI: 10.1016/j.sedgeo.2012.01.004

Sedimentary Geology 253–254 (2012) 25–46

Contents lists available at SciVerse ScienceDirect

Sedimentary Geology

journal homepage: www.elsevier.com/locate/sedgeo

Large scale facies change in the middle Eocene South-Pyrenean foreland basin: The role of tectonics and prelude to Cenozoic ice-ages

Damien Huyghe [a,b,c,*], Sébastien Castelltort [d,f], Frédéric Mouthereau [a,b], Josep Serra-Kiel [e], Pierre-Yves Filleaudeau [a,b], Laurent Emmanuel [a,b], Benoît Berthier [a,b], Maurice Renard [a,b]

[a] UPMC Univ Paris 06, UMR 7193, ISTeP, F-75005, Paris, France
[b] CNRS, UMR 7193, ISTeP, F-75005, Paris, France
[c] Laboratoire des Fluides Complexes et leurs Réservoirs, I.P.R.A. Université de Pau, BP 1155, 64013 Pau Cedex, France
[d] ETH-Zürich, Geological Institute, Sonneggstrasse 5, 8092 Zürich, Switzerland
[e] Departament de Estratigrafía i Paleontología, Facultat de Geología, Universitat de Barcelona, E-08071, Barcelona, Spain
[f] Section of Earth Sciences, University of Geneva, Rue des Maraîchers 13, 1205 Geneva, Switzerland

ARTICLE INFO

Article history:
Received 22 February 2011
Received in revised form 16 December 2011
Accepted 10 January 2012
Available online 18 January 2012

Editor: G.J. Weltje

Keywords:
Lutetian
Pyrenees
Foraminifers
Carbonates
Ice-sheets
Erosion

ABSTRACT

The present study reports a sedimentological analysis of the Guara Limestone Formation deposited during the Lutetian in the Sierras Exteriores, in the South-Pyrenean foreland basin. We provide a detailed facies analysis of the carbonates to precise the paleoenvironmental context during their deposition. We show that those limestones are mainly composed of shallow-water foraminifers and were deposited in relative shallow-water environments (<120 m) during the whole Lutetian (SBZ 13 to SBZ 16). The Guara Limestone Formation represents the last occurrence of carbonate platform in the South-Pyrenean foreland basin and disappeared definitely at the Lutetian to Bartonian transition. The demise of carbonate producers at the end of the Lutetian could be related to an increase of continental erosion, due to tectonic and/or climatic forcing. We illustrate that in the Jaca basin, this event correlates with a marked increase in subsidence rate. However, this deformation event is local and the carbonate systems in the Pyrenean foreland resisted to many deformation events during the whole basin history before. Paleobathymetric reconstructions in the Jaca basin, where shallow marine sections outcrop, suggest an increase of the amplitude of high-frequency sea-level cycles. This increase is contemporaneous with several climatic evidences, which suggest the appearance of early ice-sheets near the Lutetian–Bartonian boundary. The demise of carbonate producers seems, therefore, to be the result of a major environmental shift in the basin accompanying increased subsidence rates, switching from low nutrient oligotrophic conditions – favourable for shallow water benthic foraminifers – to eutrophic conditions due to the increase of erosion and terrigenous nutrient input associated with higher-frequency sea-level changes and river destabilization.

1. Introduction

Carbonate platforms can be deposited in different tectonic settings and can present various morphologies (e.g. Bosence, 2005). In foreland basins settings, carbonate platforms develop on the distal part of the flexural basin and show typical ramp morphologies on the distal part of the flexural basin, (Dorobek, 1995; Bosence, 2005). Based on the French–Swiss alpine foreland basin example, Sinclair (1997) defined a tectonostratigraphic model for underfilled peripheral foreland basins in which shallow-water carbonate platforms correspond to the lower unit of an underfilled trinity. In this type of setting, stratigraphic units of this trinity present a diachronous migration towards the external part of the underlying pre-orogenic strata, thus shaping a so-called basal flexural unconformity with the underlying rocks (Crampton and Allen, 1995; Allen et al., 2001). In this context, the demise of carbonates ramps results from the progressive drowning of the area of deposition illustrated by the deepening of the sedimentary facies (Sinclair, 1997; Allen et al., 2001) as the orogenic load progresses towards the foreland. The transition from an underfilled to an overfilled stage and the demise of carbonate ramps can be caused by the increase of shortening and thrust stacking including a pulse in erosional exhumation and the increase of sediment supplied from the thrust wedge or/and an increase of the flexural rigidity of the underlying cratonic plate (see Sinclair, 1997). However, attempts to reproduce the evolution of carbonate platforms in foreland basins through modelling of the stratigraphic architecture often assume the climate as stable during the period considered (Crampton and Allen, 1995; Allen et al., 2001). Our understanding of the importance of the climate factor in driving the demise of carbonate platforms in foreland basins remains therefore largely underestimated and still need to be established in such orogenic settings.

* Corresponding author.
E-mail address: damien.huyghe@univ-pau.fr (D. Huyghe).

0037-0738/$ – see front matter © 2012 Elsevier B.V. All rights reserved.
doi:10.1016/j.sedgeo.2012.01.004

Global climate has changed dramatically since the end of the Mesozoic (e.g. Zachos et al., 2001). The first order climate trend has been global cooling from a "greenhouse" system to today's "icehouse" (Zachos et al., 2008). A central observation is that geodynamic changes have been taking place during the same period, contemporaneously with the progressive climatic shift towards cooler temperatures. In particular, the Alpine–Himalayan mountain ranges have risen following the gradual closing of the Tethys ocean (Dercourt et al., 1986). The simultaneity of the evolution of climate and tectonics has prompted the question of the nature and functioning of the feedbacks between the two (e.g., Molnar and England, 1990; Raymo and Ruddiman, 1992), and thus triggered a renewal of interest for the couplings between internal and external factors and their influence on earth-surface processes.

A central question raised by Molnar and England (1990) at the heart of the debate is whether the global cooling is responsible for, or results from, the increase in relief of Cenozoic mountain ranges throughout the world and the associated increase of erosion. However, this question concerns only the very last stage of the Cenozoic. The global climate cooling which lasts since the early Eocene is most reasonably, in part, the result of the gradual rise of Cenozoic mountain ranges and the associated reorganization of ocean and atmospheric circulations, rather than its cause. As a consequence of the many orogeneses recorded during this interval, the pCO_2 lowered dramatically and has been proposed as the main factor controlling the decrease of temperatures of the Cenozoic (Pearson and Palmer, 2000; Pagani et al., 2005; Pearson et al., 2009). One fundamental outcome of this debate has been the recognition that different forcing factors can produce similar changes due to complex feedbacks between them. For example the change in the type of sedimentation and the increase of sedimentation rates observed for the last 2–4 Ma can be attributed either to a climate change or to a tectonic change, in both cases through an increase in erosion efficiency (Hay et al., 1988; Peizhen et al., 2001).

The period inaugurating the first clear step into an "icehouse" world at the Eocene/Oligocene transition is much less well documented. In many Alpine orogeny related basins, the sedimentary changes of this period are often interpreted in terms of regional tectonics changes and to their proximity to the active orogen (e.g. Sinclair, 1997). However, the last decades have seen the emergence of an increasing amount of evidence for a rich climatic history on a global scale during the early Cenozoic, allowing a better understanding of tectonic/climate relationships (Miller et al., 1987; Lear et al., 2000; Zachos et al., 2001; Tripati et al., 2005; Bohaty et al., 2009). Thus, it is fundamental to investigate whether these early Cenozoic climatic events may have dominated the sedimentary record, where there is tectonic, even in the case of foreland basins.

In addition to being of the similar age, middle Eocene carbonate platforms of the South-Pyrenean foreland basin present many similarities with the carbonate ramps of the alpine foreland basin. They were both deposited on the distal margin of the foreland basin and are mainly composed of the same carbonate producers, i.e. shallow-water benthic foraminifers (Puigdefàbregas and Souquet, 1986; Sinclair, 1997). Those carbonate platforms existed until the end of the Lutetian and their demise is considered as the response to the increase of the tectonic subsidence (Puigdefàbregas and Souquet, 1986). This episode of carbonate deposition corresponds to the lower unit of the underfilled trinity of Sinclair (1997) and constitutes a good example to study the causes of the drowning of carbonate platforms in foreland basins. In this work we document and address the demise of carbonate deposition that occurred at the Lutetian (49–41.3 Ma, Berggren et al., 1995) to Bartonian (41.3–37 Ma) boundary, prior to the major Eocene–Oligocene icehouse shift, in the South-Western Pyrenean foreland basin. Both climate and changes in tectonics could have driven this sedimentary transition. First we document the paleoenvironmental evolution during the deposition of the Lutetian calcareous Guara Formation in the Sierras Exteriores using detailed facies analysis on six sedimentary sections. The paleontological content of those deposits is studied to determine the precise age of the limestones. Second, we discuss the possible causes of the observed facies evolution. In order to do that, the tectonic subsidence is studied in the southern border of the Jaca basin. The hypothesis of a climatic forcing is tested by studying the record of high-frequency sea-level cycles as indicative of a pre-Oligocene establishment of small ice-sheets on Earth.

2. Geological setting

The Pyrenees represent the westernmost end of the Alpine–Himalayan collisional system. They form a linear mountain range resulting from the collision between the Iberian plate and the European plate starting in the late Cretaceous and lasting until the Miocene (Muñoz, 1992). The excellent preservation of foreland basin deposits particularly favours studies of syntectonic stratigraphy on mesoscale folds and thrusts. Such studies have provided a detailed picture of the tectonic development of the Pyrenean orogen (e.g. Muñoz et al., 1986; Puigdefàbregas and Souquet, 1986; Vergés and Muñoz, 1990; Puigdefàbregas et al., 1992; Vergés et al., 2002).

The South-Pyrenean foreland basin is composed of several subbasins separated by major structures perpendicular to the orogen. The Jaca basin is located in the western part of the South-Pyrenean foreland basin (Fig. 1a). Its southern border corresponds to the South Pyrenean Frontal Thrust (SPFT), which separates the Mesozoic–Cenozoic cover of the Gavarnie Unit from the nearly undeformed detrital sediments of the Ebro basin (Millán et al., 1994; Castelltort et al., 2003, Fig. 1b). As a result, it forms a clear topographic front called "Sierras Exteriores" that marks the boundary between the undeformed Ebro basin and the fold-and-thrust belt (Fig. 1c).

The sedimentary sequence in this area spans from the Triassic to the Miocene (Fig. 1b, Millán et al., 1994; Agustí et al., 2011). The evaporitic and fluviatile Triassic series are overlain by upper Cretaceous limestones and marls and Jurassic sediments are absent. A continental formation of upper Cretaceous to Paleocene age (Garumnian facies or Tremp Formation, Muñoz et al., 1986; Pujalte et al., 2009), that consists of soils, braided river and lacustrine sediments (Millán et al., 1994) marks a large scale event in the whole Pyrenean system. Above the Garumnian facies (Tremp Formation) follows the Guara Limestone Formation, a calcareous unit resistant to erosion, which forms the backbone of the frontal Sierras in the Pyrenees. The Guara Limestones are generally attributed to the middle Eocene (Puigdefàbregas, 1975; Puigdefàbregas and Souquet, 1986) and more precisely to the middle and upper Lutetian in regard to their paleontologic content (Canudo et al., 1988; Molina et al., 1988). In a more recent, but preliminary study, Rodríguez-Pinto et al. (2006) showed that the magnetochrons corresponding to the lower Lutetian are recognized at the Arguís section. Paleogeographic reconstructions (Puigdefàbregas, 1975; Plaziat, 1981; Dreyer et al., 1999) show that the Guara Limestones were deposited at the southern margin of the incipient Pyrenean foreland basin, in a position of the outer ramp of the flexural basin (DeCelles and Giles, 1996). The Guara Limestones are overlained by the Arguís–Pamplona shelfal marls and Belsué-Atarés deltaic series of Bartonian to Priabonian age, grading upwards into the Priabonian to Oligocene Campodarbe conglomeratic braided river succession. The transition from Guara Limestones to Pamplona Marls is interpreted as a sudden deepening, resulting from the southward migration of the foreland basin subsidence (Lafont, 1994). The succession ends with proximal alluvial series representing the progressive filling of the foreland basin after this initial deepening (Puigdefàbregas and Souquet, 1986; Bentham et al., 1992; Dreyer, 1993; Barnolas and Teixell, 1994; Lafont, 1994; Payros et al., 1999).

The Sierras Exteriores comprise several folds of wavelength of several kilometres which are oblique to the main orogen strike as a result of their progressive clockwise rotation due to far-field differential

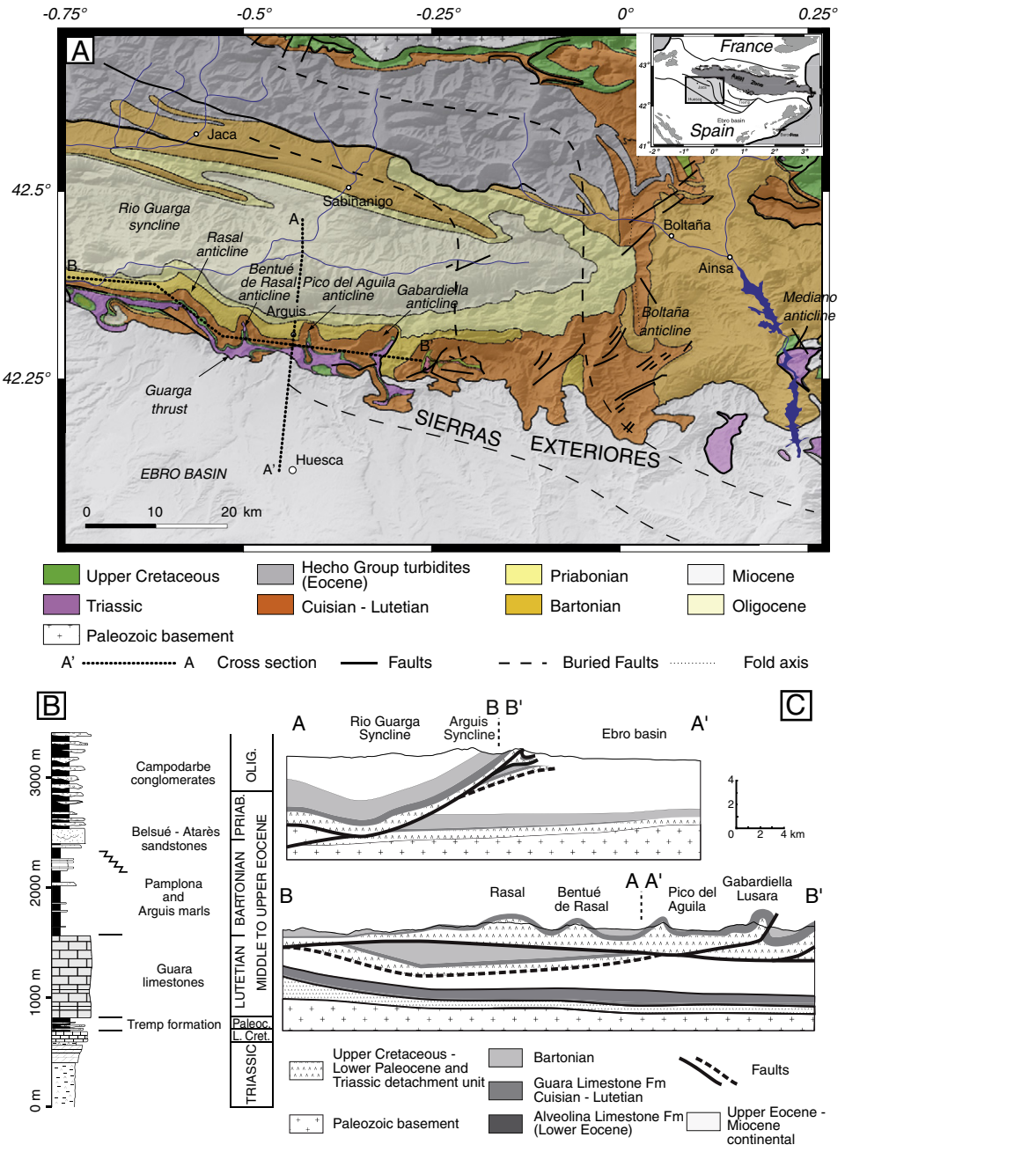

Fig. 1. (A) Geological map and location of the study area in the southern border of the Jaca basin in the Sierra Exteriores. (B) Simplified stratigraphic succession of the southern border of the Jaca basin (modified after Millán et al., 1994) and (C) Cross sections across the studied area (modified after Puigdefàbregas, 1975 and Huyghe et al., 2009). The Jaca basin is a Cenozoic piggy-back basin in which sedimentary units are detached above the basement in the Triassic evaporitic unit. The anticlines of the western Sierras Exteriores are oriented N–S and tilted to the north.

movements along the Mediano–Boltaña lateral ramp (Séguret, 1972; Millán et al., 1995; Pueyo et al., 2002; Huyghe et al., 2009). Thus, the west to east trending distribution of the Guara paleoenvironments along the South-Pyrenean front actually reflects a succession of paleoenvironments that trended southwest–northeast, i.e. from the southern stable margin towards the centre of the basin in the north, when restored in their original position. These folds plunge towards the north by about 30° as a result of their southward transport over the SPFT structural ramp emplaced in the Miocene. Thus, the transverse valleys that cut through the thrust-belt in this area provide good exposures of the foreland stratigraphy. The Pico del Aguila anticline and the Gabardiella anticline are two of these structures (Fig. 2). The first one began to grow during the late Lutetian and the second one at the end of the middle Lutetian (Millán, 1996).

3. Material and methods

3.1. Facies analysis

This work is based on the study of six sedimentary sections, covering the main part or only the upper part of the Guara Formation. These sections are located in the Sierras Exteriores, around the Pico del Aguila and Gabardiella anticlines (Fig. 2). The Arguís, Belsué and Gabardiella sections are the most complete and are located along rivers that incise the tilted limestones. These sections were chosen in order to study the paleoenvironmental evolution throughout the deposition of the Guara Limestones. The Pico del Aguila, Lusera and Rio Flumen sections cover only the upper part of the limestones, just prior to the onset of the deltaic sedimentation. The facies observed

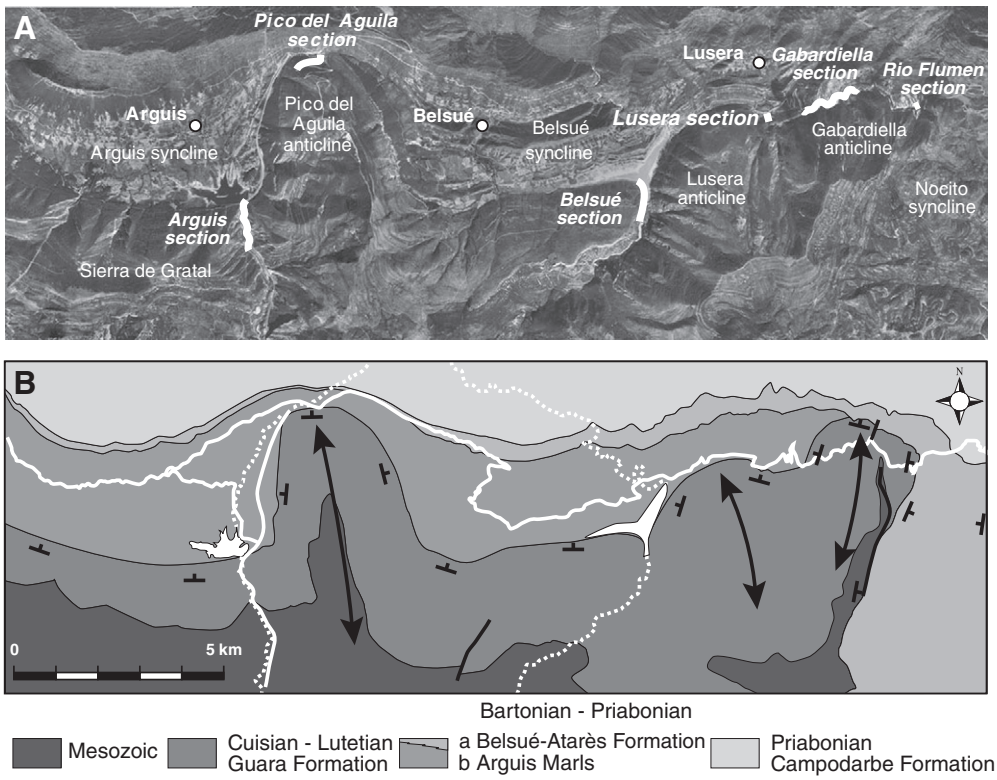

Fig. 2. (A) Aerial photo (SPOT) of the Arguís area and localisation of the sedimentary sections studied. (B) Line drawing of the main lithological–structural units of the studied area.

in these three sections are less monotonous than in the three others sections and can thus provide a more detailed evolution before the onset of the deltaic sediments. Moreover, the Pico del Aguila section is the only section accessible on a hinge of an anticline in this area, the other ones being located in the synclines or on the border of the anticlines (Fig. 2).

The sedimentary facies, the paleontological content and the sedimentary structures were studied at each section, both in the field and in thin sections, to reconstruct the paleoenvironments. Shallow-water benthic foraminifers were studied to establish the chronostratigraphic framework of the Guara Limestones in reference to the Shallow Benthic Zones (SBZ) time-scale of Serra-Kiel et al. (1998).

3.2. Tectonic subsidence calculation

With the aim of determining the possible causes of the demise of the Guara platform, the evolution of the tectonic subsidence was studied in the Sierras Exteriores. The wealth of stratigraphic and sedimentologic information available of shallow-marine series from the southern border of the Jaca basin in the area of Arguís, makes it an ideal region for backstripping the subsidence from the Triassic to the Miocene. The evolution of the sedimentation, in terms of age, thickness and depositional environment (paleobathymetries), used to calculate the evolution of the tectonic subsidence were compiled from Millán (1996), Castelltort et al. (2003) and this study for the age of the Guara Limestones. We have considered the sea-level curve of Kominz et al. (2008) to calculate the evolution of the tectonic subsidence. This parameter was calculated using a Matlab script written according to the procedure described in Allen and Allen (2005). It integrates the physical properties of the sedimentary rocks, i.e. surface porosity, porosity-depth coefficient and sediment grain mean density, according to the procedure of Allen and Allen (2005).

3.3. Accommodation calculation

In order to test the possible influence of change in climate on erosion and sedimentation, we have chosen to estimate sea level variations at high resolution, during the deposition of the Guara carbonates and the Bartonian deltaic sedimentation. Five short sections were studied for the carbonates and five others for the detrital sediments. For each detailed section, we have decompacted the sedimentary thickness and corrected for the paleobathymetry change, in order to obtain the relative sea-level variations (or accommodation) (Jervey, 1988). The paleobathymetry has been deduced from the facies model established for the Bartonian sediments by Castelltort et al. (2003) and from this work for the carbonates.

4. Results

4.1. Sedimentary facies

The six sections are composed of limestones with abundant foraminifers, with variable proportions of detrital material (Fig. 3 and 4). The most represented foraminifers are miliolids, alveolinids, *Nummulites* while *Orbitolites*, *Assilina* and *Discocyclines* are also present. Fourteen lithofacies were identified, divided in 5 facies associations, representing the main paleoenvironments of deposition. Observations are summarized in Table 1 and environmental interpretations and facies descriptions are given below. They have been differentiated on the basis of sedimentological and paleontological criteria in the field and in thin section. Reconstructions are mainly based on the distribution of the large shallow-water benthic foraminifer, whose distribution is a function of light intensity, i.e. depth, because of their association with specific symbionts (Hottinger, 1997). Thus, paleoenvironments have been deduced by comparison to the works of Molina et al. (1988), Caus and Serra-Kiel (1992), Walker and Plint (1992), Hottinger (1997), Luterbacher (1998), Geel (2000), Beavington-

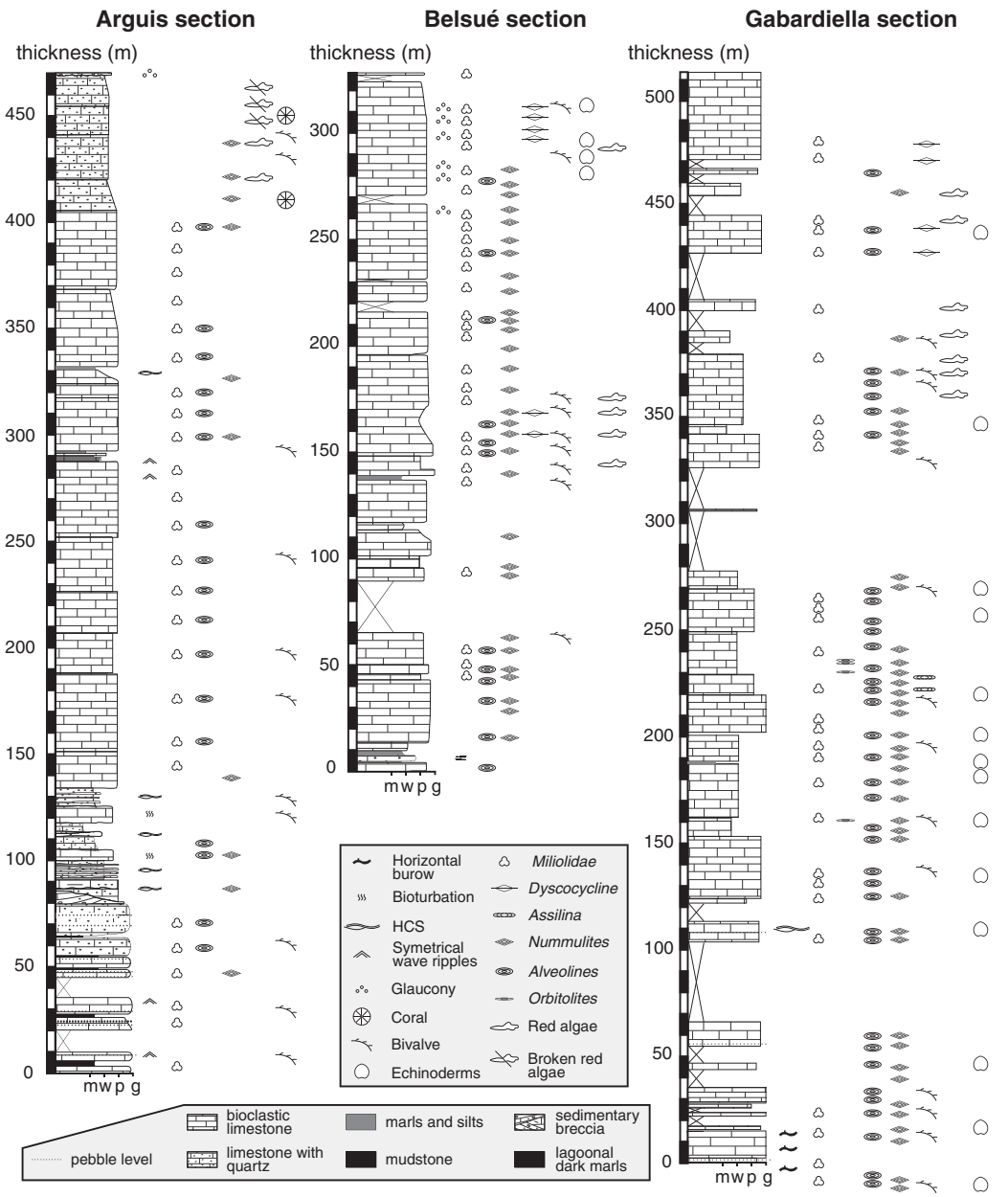

Fig. 3. Sedimentological succession and paleontological content of the Arguís, Belsué and Gabardiella sections (see Fig. 2 for precise location).

Penney and Racey (2004) and Butts (2005). All the facies indicate that the Guara Limestones were deposited in a generally shallow-water environment (<120 m).

Previous studies classified the Cenozoic carbonates platforms of the South-Pyrenees as carbonates ramps (Sinclair, 1997; Luterbacher, 1998), which are the most classical morphology of carbonate depositional systems in foreland basins (Burchette and Wright, 1992; Dorobek, 1995). Thus, paleoenvironmental zonations are defined with an inner ramp located above the Fair Weather Wave Base (FWWB), a middle ramp between the Storm Weather Base (SWB) and the FWWB and an outer ramp located under the SWB. In the Bartonian series outcropping above the Guara Limestones, Castelltort et al. (2003) proposed values of 5 ± 5 m and 60 ± 30 m for the fair-weather and the storm wave bases respectively. In this work, we chose to consider the Arabian Gulf as a modern analogue of the South-Pyrenean foreland basin, because their morphological characteristics are similar. For the modern Arabian Gulf, Walker and Plint (1992) proposed a depth of 15 m and 60 m for the FWWB and the SWB respectively. Though there is no evidence that climatic conditions have softened from the Lutetian to the Bartonian, we take into account the values of Walker and Plint (1992) and attribute a water depth of 15 ± 10 m for the fair-weather wave base during deposition of the Guara limestones and we assume 60 ± 30 for the storm wave base. Note that these values remain purely speculative and it is difficult to use modern day analogues to try calibrating ancient carbonate ramps. It is important to note that the uncertainty for the paleobathymetries increases with the water depth.

4.1.1. Inner ramp

4.1.1.1. Continental to restricted shallow-water facies. The lithofacies F1 consists of reddish sands and grey-blue silty mudstones alternating centimetre to decimetre beds. This facies is only observed in the middle of the Arguís section (at about 290 m), for a few metres. Rare miliolids and bivalves are observed in the mudstone beds, with small symmetrical wave ripples. Sand beds contain some woody debris.

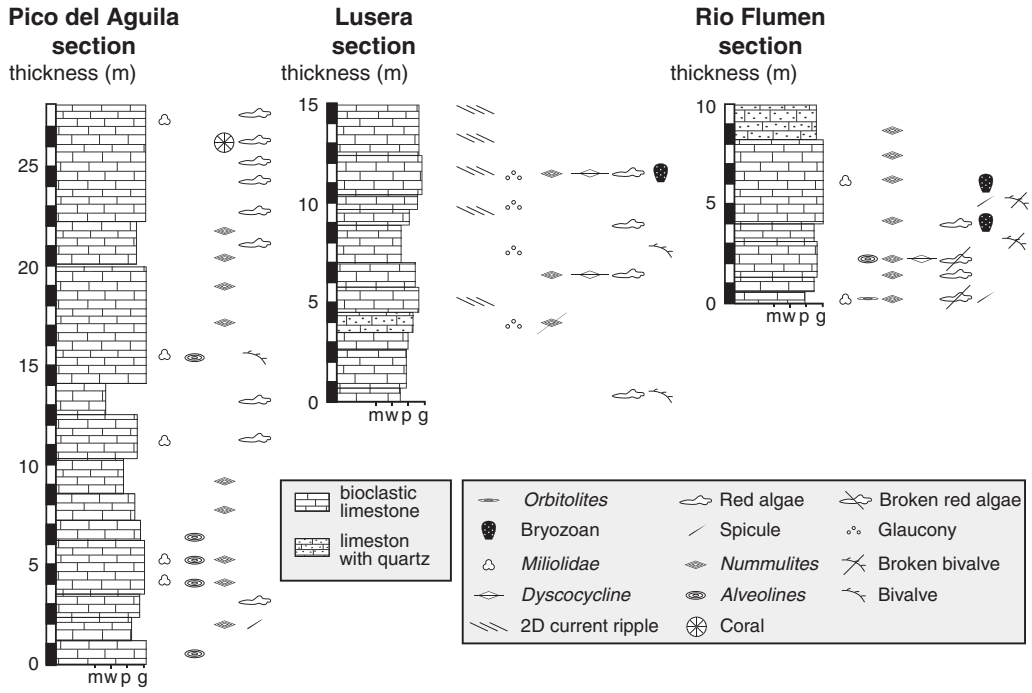

Fig. 4. Sedimentological succession and paleontological content of the Pico del Aguila, Lusera and Rio Flumen sections (see Fig. 2 for precise location).

4.1.1.2. Lagoonal facies. The lagoonal facies is comprised of two lithofacies; dark bluish marls (F2a) and thin layers of coarse conglomerates (F2b, Fig. 5a). This facies is observed in the lower part of the Arguís and Gabardiella sections and is more represented in the first one (Fig. 4).

Conglomerates appear as thin levels (few centimetres) to metric beds, included in marls or in miliolid bioclastic grainstones (Fig. 5a). They are composed of coarse rounded quartz pebbles (1 mm to 5 cm, Fig. 6c) and small (<0.5 mm) angular quartz grains (Fig. 6b and 6c) with carbonate cement. These conglomerates have a low content of fossils, but miliolids were occasionally observed in the field. Marls are finely stratified and can be nodular. They have a heterogeneous grain size and no fossils are observed (Fig. 6a). Like conglomerates, they are deposited as thin layers of several decimetres. The

Table 1
Description and interpretation of the sedimentary lithofacies identified in the six sections studied.

Facies code	Lithology	Paleontologic content	Non bioclastic content	Bioturbation	Sedimentary structures	Interpretation	Depth
F1	Dark brown silt and marls	Rare miliolids and bivalves	Quartz	Roots	Rare wave and current ripples	Shoreline	2 to +2 m
F2a	Dark fine marls	None		None	None	Lagoon	0 to 10 m
F2b	Conglomerate	None	Quartz pebbles, rare muscovite and biotite	None	None	Storm washover	0 to 10 m
F3	Grainstone	Abundant miliolids, orbitolites and alveolinids and rare molluscs, dasycladacea and characea	Quartz grains	Rare Ophiomorpha	Herring bone stratifications and symmetric wave ripple	Inner ramp	0 to 15 m
F4a	Grainstone–packstone	Dominant *Nummulites* and few miliolids, alveolinids, orbitolites and molluscs	None	None	Rare HCS	Middle-ramp	15 to 60 m
F4b	Grainstone–packstone	Dominant alveolinids and few miliolids, *Orbitolites* and *Nummulites*	None	None	Rare HCS	Middle-ramp	15 to 60 m
F4c	Packstone–wackstone	Alveolinids, *Nummulites*, miliolids, *Orbitolites* and molluscs	Quartz grains	None	Erosive base	Middle-ramp	15 to 60 m
F4d	Marls coupled packstones	Alveolinids, *Nummulites* and rare miliolids	None	None	HCS	Middle-ramp	15 to 60 m
F4e	Grainstone	Red algae	None	None	None	Middle-ramp	15 to 60 m
F5a	Packstone–wackstone	*Assilina*	None	None	None	Outer ramp	60 to 120 m
F5b	Packstone–wackstone	*Discocyclines* and few miliolids, *Orbitolites*, alveolinids, *Nummulites* and red algae	Quartz and glaucony	HCS	None	Outer ramp	60 to 120 m
F5c	Packstone–wackstone	*Discocyclines* and few miliolids, *Orbitolites*, alveolinids, *Nummulites* and red algae	Quartz and glaucony	2D current ripples	None	Outer ramp	60 to 120 m
F5d	Packstone	Wide flat *Nummulites*	None	None	None	Outer ramp	60 to 120 m
F5e	Wackstone	*Nummulites*	Quartz grains	None	None	Outer ramp	60 to 120 m
F5f	Wackstone	Broken red algae and corals	Quartz grains	None	None	Outer ramp	60 to 120 m

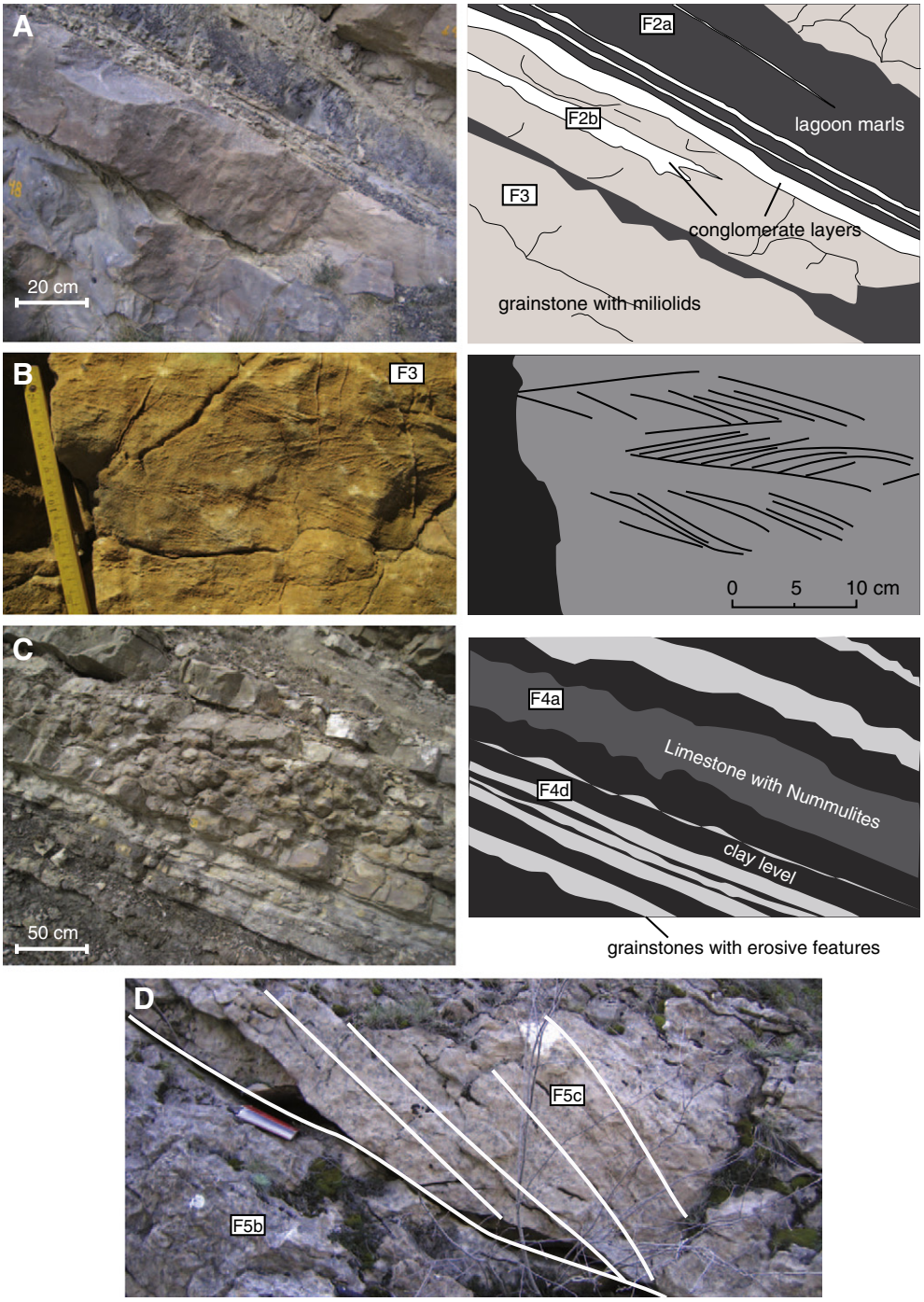

Fig. 5. Field illustrations of selected lithofacies of the Guara limestones. A: Alternation of miliolid grainstones, conglomeratic storm deposits and lagoon marls layers, B: herringbones cross stratifications in a sandy grainstone with miliolids, C: alternation between clay levels and nummulitic limestones, D: 2D current megaripples in grainstones with *Discocyclines*, *Nummulites* and red algae.

depositional environment of these two sedimentary rocks is subject to question, in particular marls can be deposited at a large range of paleobathymetries (paleobathymetries are positives starting in the sea level, i.e. 0 m). However, the conglomerate association with bioclastic grainstones (Fig. 5a) containing shallow-water benthic foraminifers like miliolids indicates very shallow-water environment (<20 m; Beavington-Penney and Racey, 2004). The alternating conglomerates and marls require rapid hydrodynamic changes. The most plausible explanation is that marls were deposited in a protected environment, such as a lagoon, isolated from the open ocean by a physical barrier, constituted by the accumulation of quartz pebbles. The thin conglomerate layers observed in association with the marls could then be interpreted as originating from littoral bars reworked and re-deposited in a lagoon under the action of storms. The heterogeneity of the grain size of the conglomerates supports the idea of catastrophic events.

4.1.1.3. Carbonate inner ramp facies. This facies association (F3) is represented by grainstones with a very rich paleontologic content. Fossils of this facies are dominated by shallow-water benthic foraminifers, in particular miliolids, alveolinids and *Orbitolites* (Luterbacher, 1998). Broken bivalves, mainly oysters, and gastropods, can be found in these facies.

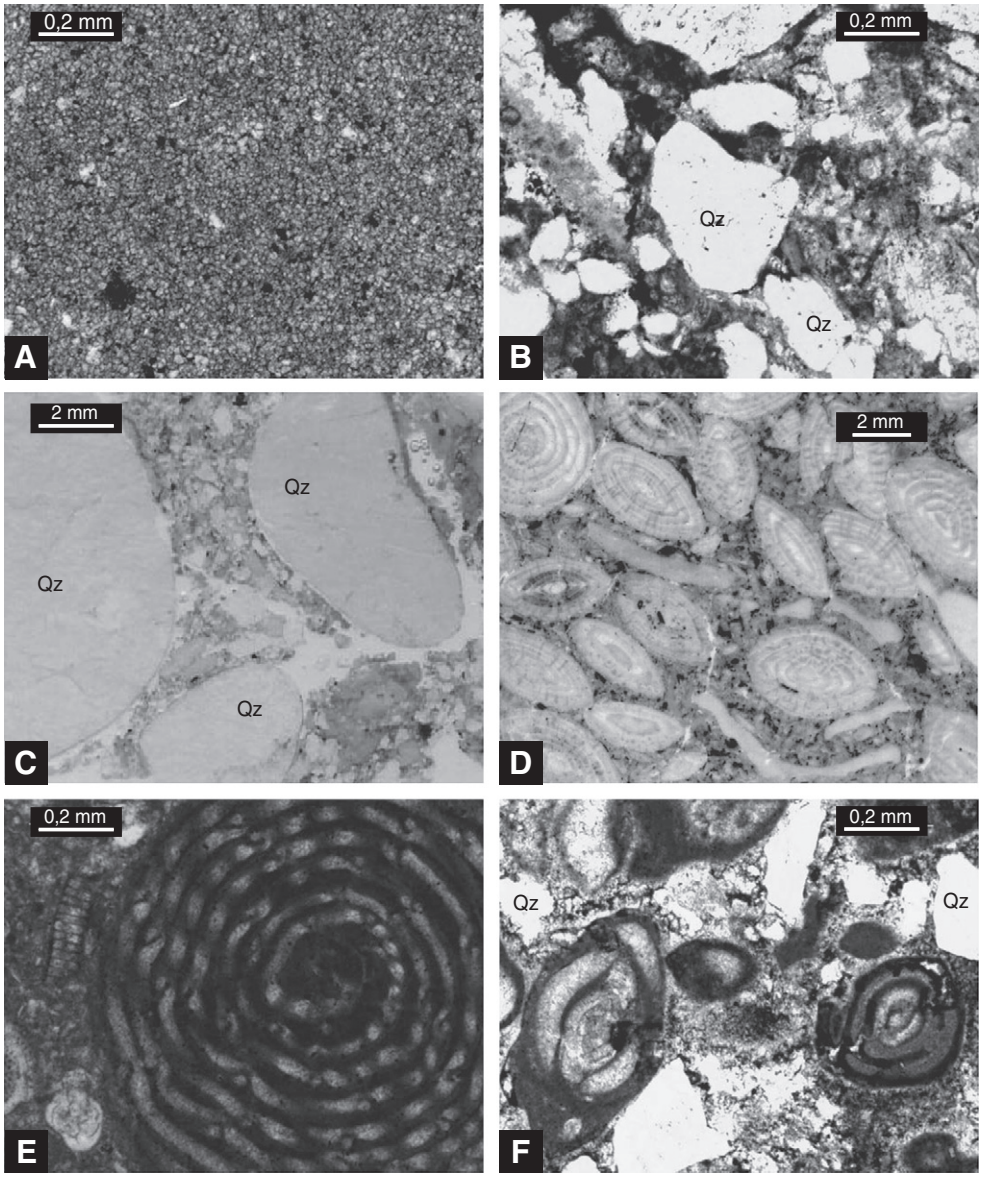

Fig. 6. Photographs of microfacies of the Guara limestones. A: marls deposited in lagoon environment (F2a); B: thin fraction of conglomerate layers composed of angular quartz grains (Qz) with carbonate cement (F2b); C: quartz round pebbles and small quartz grains composing the conglomerate of the base of the Guara formation (F2b); D: grainstone with *Nummulites* (F4a); E: packstone with *Alveolina* (F4b); F: grainstone with miliolids, angular quartz grains and bioclasts (F3).

Moreover, rare *Dasycladacae* and charophytes are observed in thin sections. The bioturbation is mainly represented by *Ophiomorpha*, *Skolithos* and *Teredolites* traces. In the lower part of the Arguís section, these grainstones contain variable amounts of small angular quartz grains, with similar grain size and morphology as those observed in the conglomerates (Fig. 6f). Rare muscovite and biotite crystals are observed in thin section. Sedimentary structures are sparse but centimetre to decimetre scale and herringbone cross-stratifications can be observed in places (Fig. 5b).

The paleontologic content (miliolids, *Orbitolites* and green algae), burrows, lithology and sedimentary structures indicate shallow-water environment, probably located close to the continent because of the presence of continental green algae. Foraminifers observed in these paleoenvironments are often associated with sea grasses, which are the preferred substrate of many those organisms living between the mean sea level and ~30 m (Fig. 7; Brasier, 1975).

Moreover, the general absence of mud in the herringbones cross-stratifications can be attributed to possible deposition in intertidal environments. The hydrodynamism is interpreted to be very variable, lithologies indicating alternations between restricted calm environments and very high-energy environments with bipolar current directions and association of very various fossils living at different depths. The depositional environment of this facies association is thus attributed to the inner ramp, influenced by storms and tides.

4.1.2. Middle ramp

Luterbacher (1998) interpreted the Paleogene calcareous deposits of the Southern-Pyrenean foreland basin containing *Nummulites* to be deposited in middle ramp environments. Grainstones and wackstones with high concentration of nummulitids (F4a) constitute one of the most abundant facies of the Guara Limestones in the Sierras Exteriores. In these limestones, *Nummulites* can be found with variable proportions of miliolids, orbitolites and alveolinids, which implies an exportation of these fossils, probably because of the influence of storm process.

Packstones, with a large proportion of alveolinids, with a reduced concentration of miliolids, *Orbitolites* and *Nummulites* are observed too (F4b). It is the most represented facies in the Arguís section,

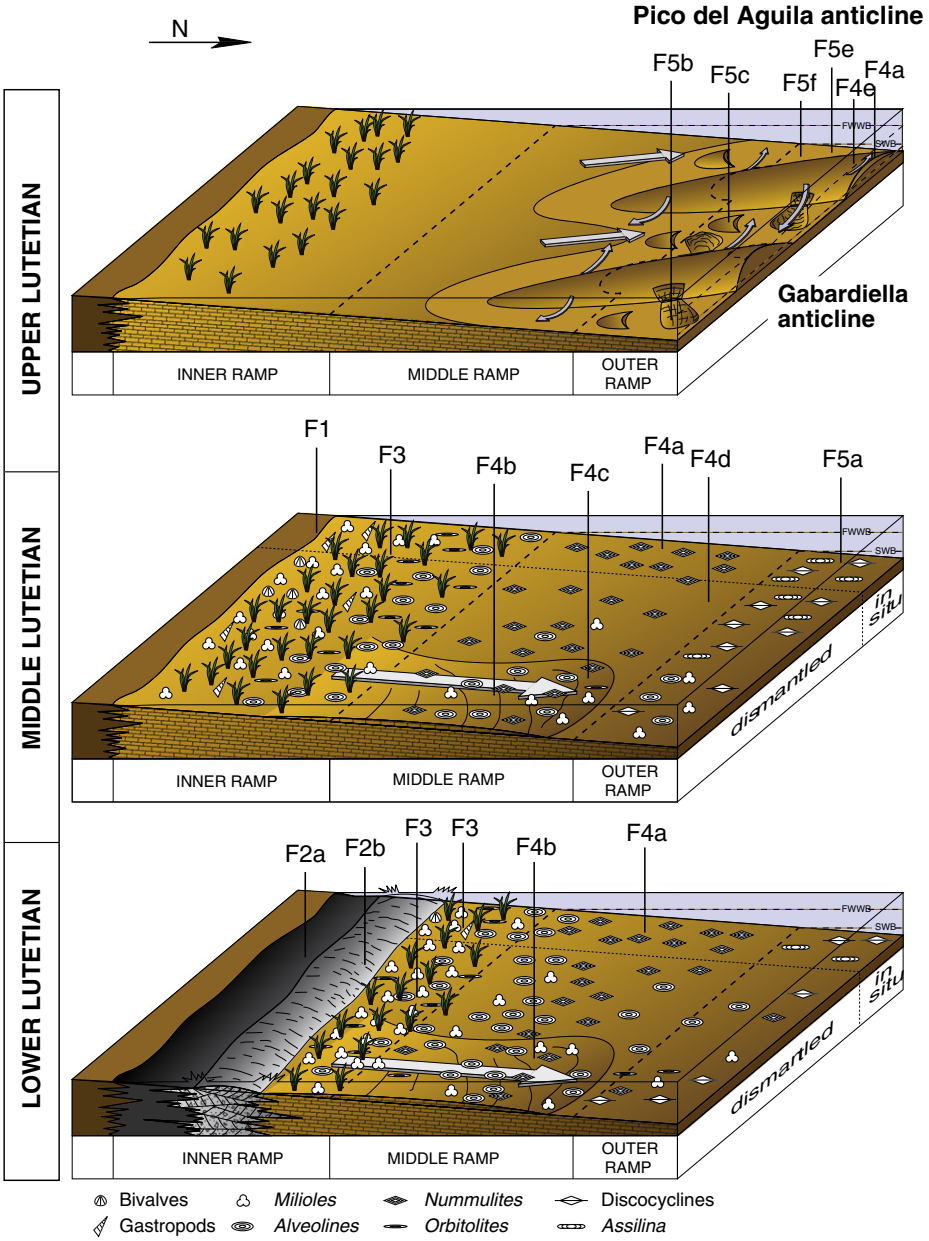

Fig. 7. Paleoenvironmental evolution during the deposition of the Guara limestones in the Sierras Exteriores and location of the different lithofacies. Ages are deduced from the content in shallow-water benthic foraminifers in reference to the SBZ time scale of Serra-Kiel et al. (1998). The paleolandscape was that of a ramp with a bar and lagoon during the lower Lutetian and a monoclinal ramp during the middle Lutetian. During the late Lutetian, the Pico del Aguila and Gabardiella anticlines began to grow. No vertical and horizontal scale. FWWB for fair weather wave base and SWB for storm wave base.

from about 150 m to 320 m. No siliciclastic particles are observed and the only sedimentary structures observed in the field are hummocky cross stratifications (HCS), implying the influence of storms. According to the zonation of Luterbacher (1998), this facies association records shoreface environments in situ when *Alveolina* dominates, and upper offshore environments when *Nummulites* are mixed with *Alveolina* and miliolids resulting from reworking by storms. This kind of facies could even represent the morphology of a sedimentary breccia in the lower part of the Arguís section (F4c). These packstones with alveolinids can also represent the morphology of multi-decimetres thick levels of alternating layers of marls without fossils and marls with storm erosive bases (F4d; Fig. 5c).

In the Pico del Aguila and Rio Flumen sections, localized layers of grainstones, with large amounts of red algae, alternating with layers of grainstones dominated by *Nummulites*, are also observed (F4e).

4.1.3. Outer ramp

According to Luterbacher (1998) *Assilina* and *Discocyclines* of the South-Pyrenean foreland basin during the Paleogene, characterize the outer ramp. *Assilina* are only observed in the middle part of the Gabardiella section (F5a). *Discocyclines* are present in the upper part of the Belsué, Lusera, Gabardiella and Rio Flumen sections, associated with other fossils, like miliolids, red algae, echinids and alveolinids. These facies sometime contain a significant proportion of glauconite (F5b; Fig. 3 and 4). Large wavelength 2D ripples with a northward direction are observed in the Lusera section within these lithofacies (F5c) and could correspond to deep dunes (Fig. 5d).

Near the top of the Gabardiella section, a large, wide and flat species of *Nummulites*, *Nummulites millecaput* is observed (F5d). This species of *Nummulites* characterizes deep and calm environments, at the lower limit of the photic zone (Beavington-Penney and Racey, 2004).

In the Arguís area, the upper part of the section is comprised of silty wackstones with large *Nummulites* (F5e), overlain by fine wackstones with red algae debris and some coral fragments (F5f). It is hard to give a precise depth of deposition for these facies, but by comparison with the contemporaneous deposits of the Guara Limestones in the Belsué syncline, we can propose that they were deposited in an outer ramp environment.

4.2. Biostratigraphy and correlation between the studied sections

We have chosen the Arguís section as our reference to establish a chronostratigraphical framework, because the paleontological content of this section has been studied by Canudo et al. (1988) and Molina et al. (1988) and preliminary paleomagnetic studies were performed by Rodríguez-Pinto et al. (2006). Moreover, the age of the Bartonian deltaic sediments is well constrained in the Arguís syncline (Millán et al., 1994; Hogan and Burbank, 1996; Sztràkos and Castelltort, 2001; Castelltort et al., 2003; Rodríguez-Pinto et al., 2006).

We have identified the content of shallow-water benthic foraminifers to precise the Lutetian age of this formation with reference to the Shallow Benthic Zones of Serra-Kiel et al. (1998). Thirteen points located in Fig. 8 were analysed in the Arguís section. The samples 1 and 2 contain *Alveolina callosa* Hottinger, 1960 and *Alveolina tenuis* Hottinger, 1960. These species according to Hottinger (1960) and

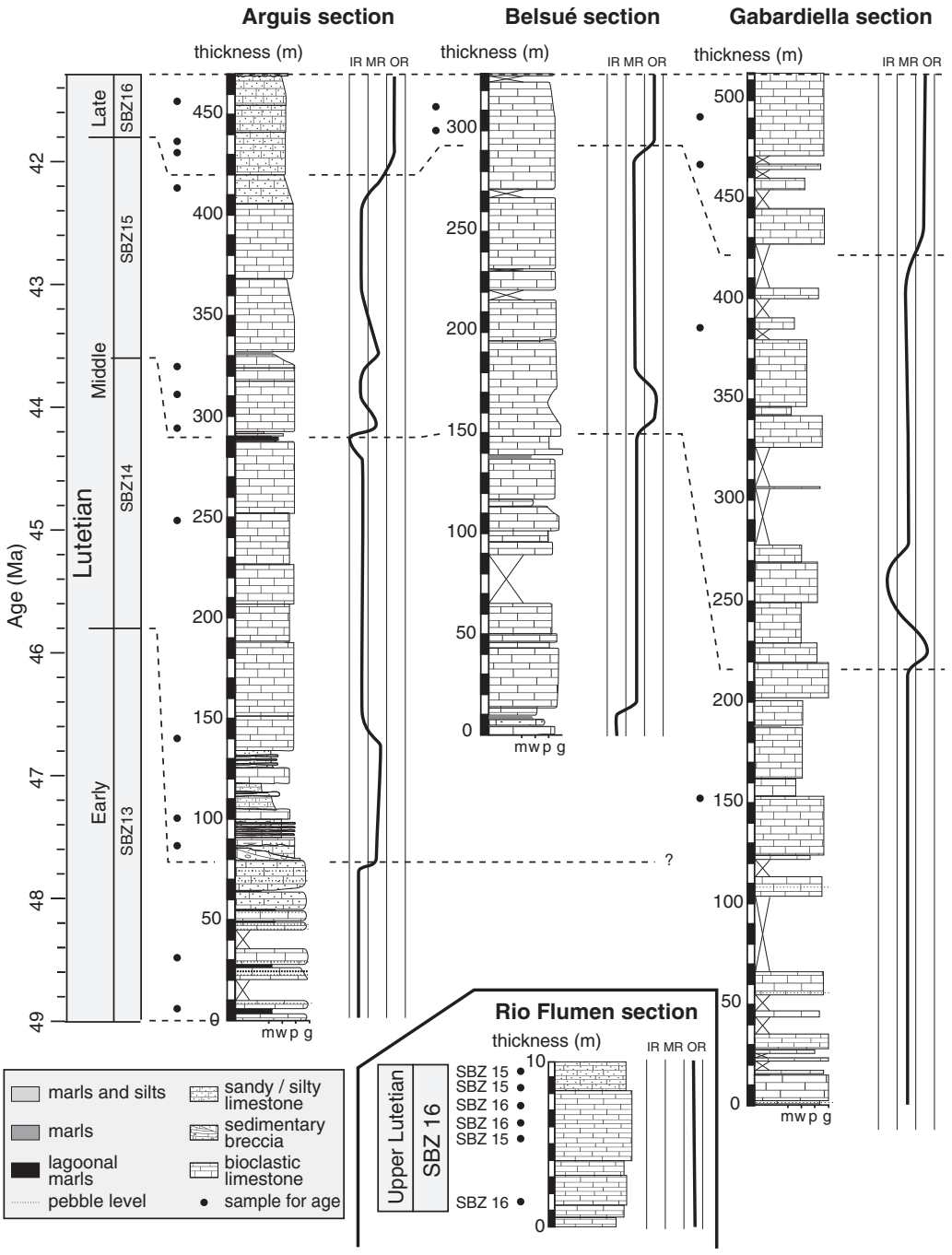

Fig. 8. Age model and paleo-water depth evolution for the Guara Limestone Formation. Ages are determined from the foraminiferal content relative to the Shallow Benthic Zones (SBZ) time scale (Serra-Kiel et al., 1998). The Guara Limestone Formation in the Arguís section covers the whole Lutetian, going from SBZ 13 to SBZ 16. Paleo-water depths are deduced from the facies model. The Pico del Aguila and Rio Flumen sections are too small to be presented in this figure and present low biostratigraphic interest. IR for Inner Ramp, MR for middle ramp and OR for Outer Ramp. Dotted lines represent correlations between the different sections, based on biostratigraphic and paleo-water depth evolutions.

Hottinger and Drobne (1988) indicate an age of early Lutetian or SBZ 13. The samples 3–6 contain *Alveolina munieri* Hottinger 1960, *Nummulites aspermontis* Schaub 1981, *Nummulites beneharnensis* De La Harpe in Rozlozsnik 1926, *Nummulites discorbinus* Schlotheim 1820, *Nummulites migiurtinus* Azzaroli 1950 and *Assilina spira spira* De Roissy 1805. This larger foraminifer association indicates middle Lutetian 1 according to Hottinger and Drobne (1988), Schaub (1981) or SBZ 14. The interval from sample 7 to 10 contains *Nummulites crassus* Boubée 1831 and *Nummulites* aff. *deshayesi* D'Archiac and Haime 1853 that indicates middle Lutetian 2 according to Schaub (1981) or SBZ 15. Finally, the samples 11–13 contain *Nummulites deshayesi* D'Archiac and Haime 1853, which indicates an age of late Lutetian or SBZ 16 according to Schaub (1981) and Serra-Kiel et al. (1998).

In the Belsué section, we have only identified *N. deshayesi* at the top of the section, which indicate the SBZ16 or the late Lutetian. Concerning the Gabardiella section, few data are available (Fig. 8).

In the short sections of the Pico del Aguila and Lusera, *N. deshayesi*, which indicates the SBZ16, i.e. the late Lutetian, was identified. Concerning The Rio Flumen section, more foraminifers are identified. In the bottom of the section, we found *N. deshayesi* (SBZ 16) and *N. beaumounti* (SBZ 16). At top of the section, *Nummulites* aff. *deshayesi* and *Nummulites* cf. *crassus*, characteristic of the upper middle Lutetian, or SBZ 15, are identified (Fig. 8).

Those results combined with the existing data already constraining the age of the Pamplona Marls (Millán et al., 1994; Hogan and Burbank, 1996; Sztràkos and Castelltort, 2001; Castelltort et al., 2003; Rodríguez-Pinto et al., 2006) allow a precise estimation of the age of the upper part of the Guara Limestones, at the Lutetian–Bartonian boundary in the Sierras Exteriores. Concerning the base of this formation in the Arguís section, existing studies are in disagreement. Previous biostratigraphic studies have dated its base at the beginning of the middle Lutetian, whereas magnetostratigraphic studies have recognized the lower Lutetian with the identification of the magnetochron C21 corresponding to the beginning of the lower Lutetian (Rodríguez-Pinto et al., 2006). In the present study, we have also observed foraminifers characterizing SBZ 13, i.e. the lower Lutetian. By combining all these data, we can thus propose that the age of the base of the Guara Limestones corresponds to the beginning of SBZ13, i.e. the beginning of the Lutetian (49 Ma).

The study of the paleontological content and the facies evolution of the Arguís, Belsué and Gabardiella sections highlights that the paleo-water depth followed the same evolution in the three sections (Fig. 8). This evolution, combined to the biostratigraphic ages allows a correlation between the six sections. Paleo-water depths are relatively low at the bottom of the Arguís section, with inner ramp facies. The paleo-water depth is relatively constant except around the transition between the SBZ 14 and the SBZ 15, which constitute a strong element of correlation between the sections (Fig. 8). At the top of the three sections, a deepening is recorded to the outer ramp environment, which agrees with a regional increase of the subsidence in the southern border of the basin (Lafont, 1994). However, despite this similarity in the paleo-water depth evolution during the Lutetian, the absolute depth is not the same at each locality for the same age. The explanation could be found in the progressive tectonic transport above an ~south-directed ramp over the foreland sedimentary series and the clockwise rotation of this area since the Bartonian (Pueyo et al., 2002; Huyghe et al., 2009). As a consequence, the repartition of the studied outcrops during the Lutetian was not the same as today and their relative disposition, that is currently an east–west alignment, was different during the Lutetian and thus not parallel to the paleo-coastline due to the post Lutetian clockwise rotation of the studied area. Thus, during the Lutetian, the Belsué and Gabardiella sections were located in deeper environments compared to the Arguís section.

4.3. Paleoenvironmental evolution

4.3.1. Lower Lutetian

During the deposition of the lower part of the Guara Limestones, marls are observed in association with conglomerates. These facies are interpreted to be deposited in a lagoonal environment, isolated from the open oceanic domain by sedimentary bars build by the accumulation of coarse quartz grains (Fig. 7). This detrital material may have been introduced to the sea by a clastic source point such as a river. The heterogeneity of the grain size of the quartz (coarse rounded pebbles and small angular grains) and the presence of muscovite and biotite minerals suggest that this detrital material could have been supplied by the erosion of magmatic rocks. Nevertheless, the size and the morphology of the coarse pebbles suggest a possible reworking of detrital material from older sedimentary rocks of the underlying Cretaceous–Paleocene Garumnian facies, which were eroded southwards of the studied successions in the foreland area (Dreyer et al., 1999).

On the outer part of the barrier, the sedimentation was dominated by the deposition of shallow-benthic foraminifers and molluscs. In the sections studied, we only observe fossils and lithologies indicating the inner ramp to the middle ramp. Foraminifers observed such as orbitolites indicate the presence of seagrass and mud-free substrates (Geel, 2000).

4.3.2. Middle Lutetian

During the middle and upper Lutetian, the sedimentary barrier seems to have disappeared because quartz pebbles and lagoon marls are no longer recognized in the carbonates. The disappearance of the coarse detrital material is probably a consequence of a rise in sea level observed all along the Guara Formation. Due to this transgressive trend, the clastic source might have been pushed a long way back towards the hinterland and caused the reduction of the clastic influx to the marine domain, or even covered by the limestones if we consider the Garumnian formation as the main source.

The morphology of the Guara formation was thus a simple proximal–distal profile opened towards the sea, and sedimentary facies observed reflect alternation between the inner ramp and the outer ramp according to each section (Fig. 7). Shallow-water benthic foraminifers from different depths are often mixed, which implies significant reworking of bioclastic material and a sedimentation dominated by storm processes in this area.

4.3.3. Late Lutetian

The paleolandscape of the studied area was significantly influenced by the onset of growth of the Pico del Aguila and Gabardiella anticlines during the late Lutetian. This period is covered by the six sections and is thus the interval when most data are available in our study. The six sections display a great diversity of facies.

In the section of Arguís, the texture consists of wackstones–packstones, with large and small rounded *Nummulites*. The upper part is characterized by red algae fragments in a dark calcareous silty matrix. The Pico del Aguila section is the only one accessible on the hinge of an anticline, the others being located in the synclines. In this section, we observe grainstones with large and small nummulitids and rare alveolinids, miliolids and bivalves. The last levels of this section are comprised of grainstones with red algae and some corals. In the Belsué section, we found packstones with glauconite. These deposits contain various fossils, like miliolids, nummulitids, discocyclines, bivalves, echinids and some red algae. These fossils have theoretically different ecological preferences. Some, like miliolids and oysters, live in the inner ramp, whereas discocyclines are observed in deeper environments, at the lower limit of the photic zone (Luterbacher, 1998). Thus, those associations of fossils are the result of transportation of material. The same kinds of deposits are observed in the Lusera and Gabardiella sections, revealing transportation of fossils at

important water depth (<90 m). Moreover, the presence of a large (<5 cm) flat species of *Nummulites*, *N. millecaput*, at the top of the Gabardiella section, implies a deep and quiet environment at the limit of the photic zone. The presence of 2D megaripples at the top of the Lusera section suggests the formation of deep-water dunes. These structures may result from a unidirectional current formed between the two anticlines with a direction to the north (Fig. 7).

In the Rio Flumen section, we found grainstones with rich levels of large and small *Nummulites* and red algae. Sparse bilvalves shells, spicules of echinoderms, miliolids, *Orbitolites*, *Discocyclines*, *Alveolina* and bryozoan are also observed in thin sections, which also suggest a transportation of fossils. Fining upwards sequences are also observed in thin sections, suggesting micro-turbiditic deposits. The biostratigraphic analysis of the content in shallow-water benthic foraminifers is in good agreement with a dismantlement of fossils too. Indeed, we have identified an association of foraminifers characterizing SBZ 16, i.e. the upper Lutetian, with fossils from the SBZ 15, i.e. from the upper middle Lutetian (Fig. 8). The most plausible scenario to explain this configuration is that in situ sedimentary deposits at the Rio Flumen section occurred contemporaneously with the erosion and exportation of the sediments initially deposited on the hinge of the Gabardiella anticline.

Thus, during the late Lutetian, in situ deposits were eroded on the anticlines, whereas in the synclines, sediments correspond to a remobilization of mixed particles destabilized by the growth of the anticlines alternating with in situ sedimentation (Fig. 9). Siliciclastic particles, fed by the arrival of the delta of Arguís and glauconite were only deposited in the synclines. Miliolids are observed on the border of the Gabardiella syncline, whereas *Nummulites* are observed on the hinge of the Pico del Aguila anticline. It suggests that the Gabardiella anticline was probably more elevated than the Pico del Aguila anticline, the top of the first one being located below the FWWB and the second one between the FWWB and the SWB (Fig. 9). It seems that at the scale of the fold, the tectonics played a role only in the distribution of the facies, but not on the nature of the sedimentation, i.e. carbonates or detrital.

5. Cause of the demise of the carbonate platforms

5.1. A local or a regional evolution?

The integration of the biostratigraphic data obtained for the Guara carbonate Formation and the data available for the deltaic sedimentation allows us to establish a precise tectono-chronostratigraphic framework in the Sierras Exteriores during the middle Eocene (Fig. 10). The ages obtained for the top of the Guara carbonate Formation all agree with an upper Lutetian age (SBZ 16), even if the topmost of each section was not precisely dated. However, SBZ 16 is one of the shorter SBZ and has duration of 0.3 Ma (Serra-Kiel et al., 1998). It was not possible to date the boundary between carbonates and clastic sediments, because no reliable biostratigraphic shallow sea-water foraminifers were available in the Arguís and Belsué sections or well preserved in the Gabardiella section. However, the top of the Rio Flumen, Lusera and Pico del Aguila sections are well dated and belong to SBZ16. Moreover, previous magnetostratigraphic studies have assigned an upper Lutetian (SBZ16) age to the top of the Arguís section and a lower Bartonian age to the base of the marls. Lithostratigraphic correlations have assigned the same age to the base of the detrital formations from the Arguís syncline to the western flank of the Gabardiella anticline (Castelltort et al., 2003). This indicates that the transition between the carbonates and the detrital Arguís and Belsué–Atarès Formations happened at the Lutetian–Bartonian transition, with the appearance of mixed detrital carbonate sedimentation in the synclines, since the upper Lutetian.

In order to check the regional or local character of the carbonate to clastic transition highlighted in the Sierras Exteriores, we have established synthetic paleogeographical maps for the Lutetian and the Bartonian in the whole South-Pyrenean foreland basin (Fig. 11). These maps summarize information from the works of Séguret (1972), Puigdefàbregas (1975) and Mutti (1977) for the Jaca basin, Plaziat (1981) for the whole South-Pyrenean basin, Lanaja (1987) for the buried sediments of the Jaca and Ebro basins, Millán (1996) and this study for the southern border of the Jaca basin, Payros (1997) and Payros et al. (1999) for the south-western foreland region of Pamplona, Bentham et al. (1992), Nijman (1998) Dreyer et al. (1999) and Caja et al. (2010) for the Ainsa basin, and Lopez-Blanco (2002), Serra-Kiel et al. (2003) and Vera (2004) for the eastern foreland. In addition we have also used the geological maps of the Arguís area (José et al., 1951), Catalunya (Losantos et al., 1989) and our own field data. We have reported, where it was possible, the facies of the upper Lutetian and the lower Bartonian on the modern map of the Pyrenees. Where this information was not available, we have extrapolated from the facies encountered during the middle Lutetian and the upper Bartonian.

The obtained paleogeographic map for the Lutetian (Fig. 11a) highlights the presence of several carbonate environments on the southern border of the basin (Guara carbonate Formation) and in its eastern part (Tavertet/Girona Limestone Formation), far from detrital supply. These carbonate platforms and ramps coexisted with clastic sedimentation, essentially sourced in the growing Pyrenees and accumulating in the underfilled Jaca basin (Hecho Group, Mutti, 1977) and with the already filled Tremp–Graus (Escanilla and Cajigar formations; Beamud et al., 2003) and Ainsa basins (Sobrarbe and Escanilla formations; Beamud et al., 2003). Clastic sedimentation at this time also took place on the western border of the Catalan Coastal Ranges (La Salut sandstones and Les Bruixes conglomerates, Lopez-Blanco, 2002).

In contrast, the paleogeographic map during the Bartonian (Fig. 11b) shows a complete reorganization of the sedimentary landscape, with only detrital and minor mixed sedimentation and a total absence of continuous marine carbonate ramp deposition. A major uncertainty in those paleogeographic maps refers to the connexion between the marine eastern part of the foreland basin and the Jaca basin. But this has no effect on the disappearance of the carbonate platforms and ramps. In the north Pyrenean foreland basin, the sedimentation has been continental since the early Eocene (Plaziat, 1981).

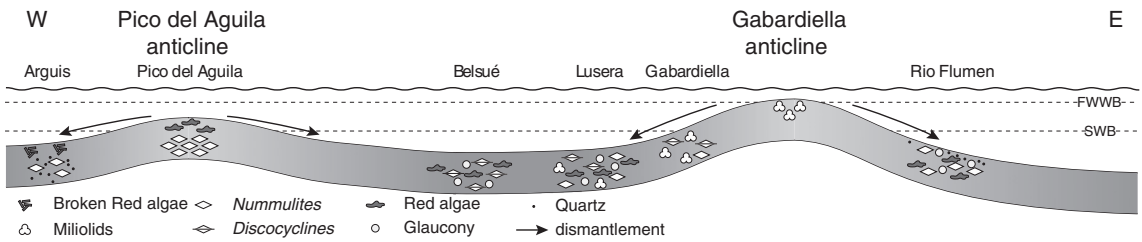

Fig. 9. Illustration of the influence of the growth of the Pico del Aguila and Gabardiella anticlines on the repartition of sedimentary facies during SBZ 16 (upper Lutetian). Arrows represent the direction of dismantlement of the particles from the hinge of the anticlines to the synclines. FWWB for fair weather wave base and SWB for storm wave base. No vertical scale.

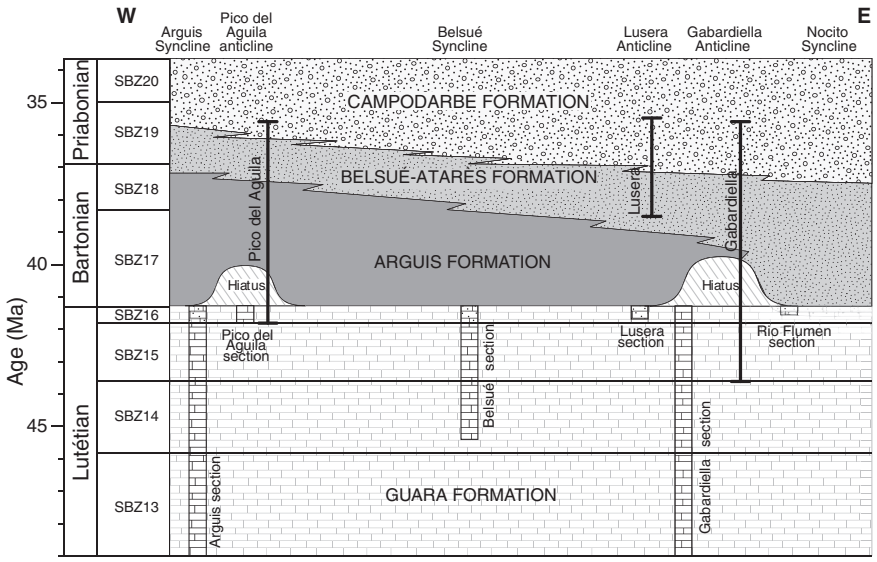

Fig. 10. Chronostratigraphic framework of the Sierras Exteriores during the middle Eocene and timing of growth of the anticlines (after Millán, 1996). The stratigraphic extension of the Arguís, Belsué-Atarès and Campodarbe Formations are from Canudo et al. (1988), Molina et al. (1988), Millán (1996) and Castelltort et al. (2003).

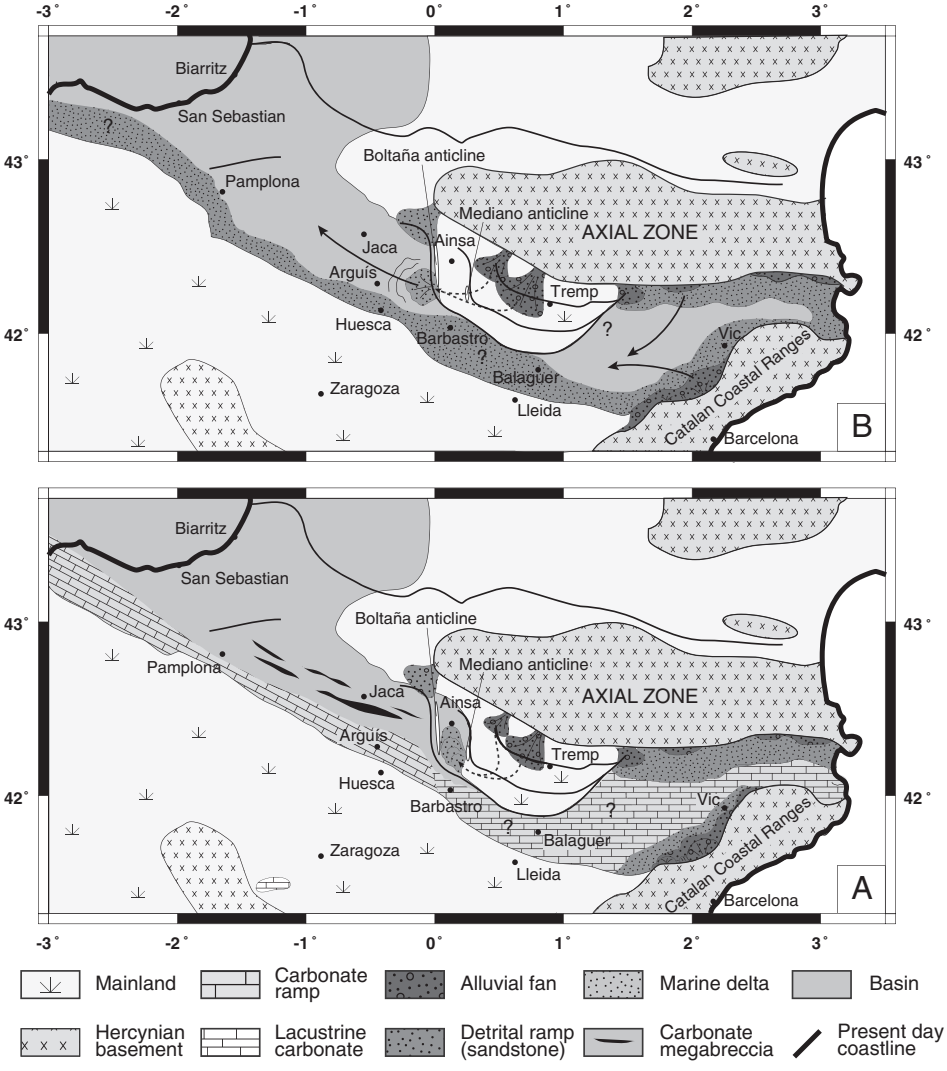

Fig. 11. Paleogeographic maps of the South-Pyrenean foreland basin during the Lutetian and the Bartonian. After Puigdefàbregas (1975), Plaziat (1981), Lanaja (1987), Bentham et al. (1992), Millán (1996), Payros (1997), Nijman (1998), Payros et al. (1999), Dreyer et al. (1999), Lopez-Blanco (2002), Serra-Kiel et al. (2003), Vera (2004), Geologic Map of Catalunya at 1:250,000 and field data.

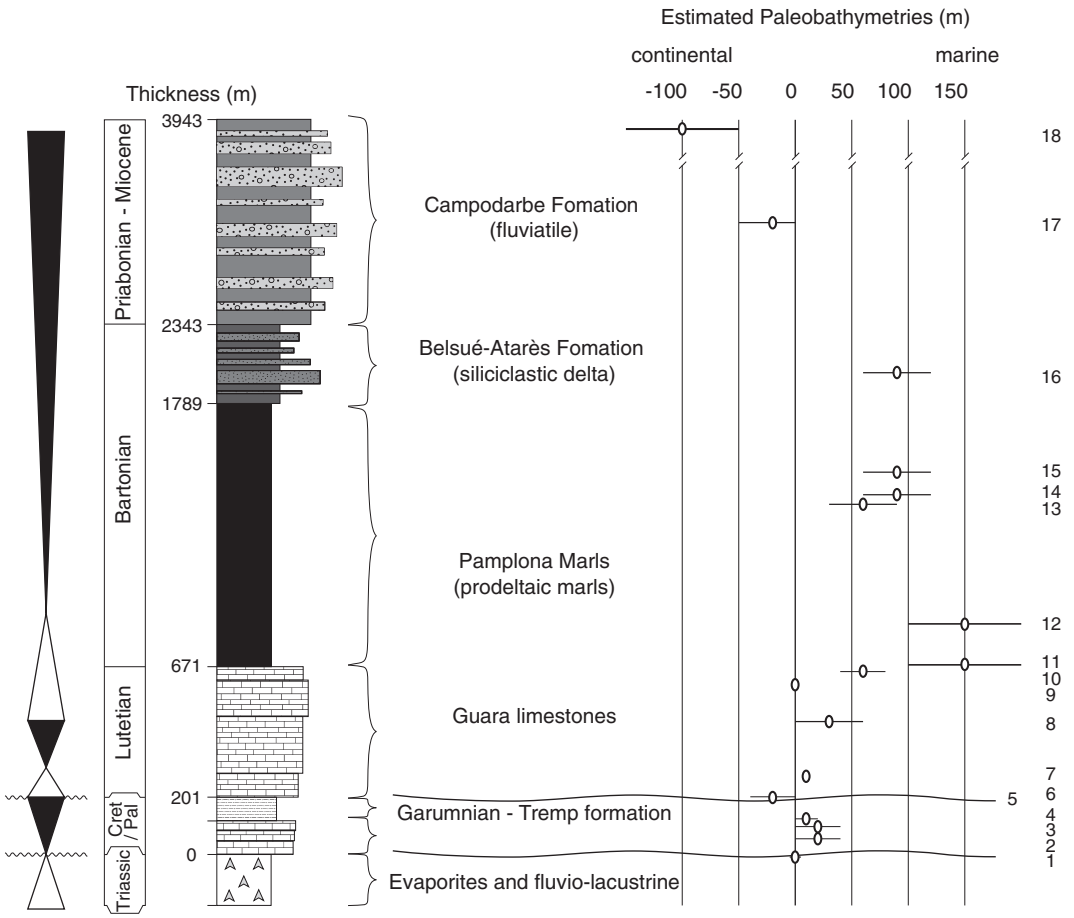

Fig. 12. Synthetic sedimentologic evolution in the Sierras Exteriores near Arguís. Thickness, ages and paleobathymetries are estimated from Millán (1996), Castelltort et al. (2003) and this work. Numbers on the right correspond to the layers used to calculate the tectonic subsidence (see Table 2).

The main carbonate formations that existed until the end of the Lutetian were the Tavertet/Girona Limestone Formation in the eastern Ebro basin and the Guara carbonate Formation in the southern border of the Jaca basin (Puigdefàbregas and Souquet, 1986; Vergés et al., 1998; Serra-Kiel et al., 2003). The age of the Tavertet/Girona Limestone Formation, which succeeded the Cadì-Orpì, and Penya Formations after their migration to the south in response to the migration of the tectonic subsidence (Vergés et al., 1998), is well constrained by biostratigraphic (Samsó et al., 1994; Serra-Kiel et al., 2003) and magnetostratigraphic constraints (Burbank et al., 1992; Bentham and Burbank, 1996) data. Its base and top become younger to the south, but the first strata are dated to be early Lutetian, while the top was deposited to the end of the late Lutetian (end of SBZ 16; Fig. 13). In the Sierras Exteriores, we have shown that the age of the top of the Guara carbonate Formation was synchronous with the SBZ 16–SBZ 17 transition i.e. with the Lutetian–Bartonian boundary. Concerning the western part of the foreland basin, in the area of Pamplona and to the west, the last carbonate platforms also existed until the end of the Lutetian (Plaziat, 1981; Puigdefàbregas and Souquet, 1986; Payros 1997). During the Bartonian, carbonate platforms of typical Lutetian morphology ceased to exist and carbonate deposition was restricted to small *Nummulites* bars and patch reef growths (Puigdefàbregas and Souquet, 1986).

5.2. Potential causes for the disappearance of the carbonate producers

The Guara Limestone Formation is mainly comprised of shallow water benthic foraminifers, which are sensitive to several parameters such as water transparency and nutrients availability – both influenced by clastic input – and have very strict environmental preferences (Hottinger, 1983; Hallock and Schlager, 1986; Racey, 1992). Biomineralization of calcium carbonate by benthic foraminifers can often happen in oligotrophic and warm water and in illuminated environments (Hottinger, 1983; Racey, 1992), conditions that are present during the Lutetian in the Pyrenees. Indeed, these species live with symbiotic algae, which control their environmental and bathymetric distributions (Leutenegger, 1984). Moreover, because of their symbionts, many shallow-water benthic foraminifers can only live under nutrient-deficient oligotrophic conditions (Hallock and Schlager, 1986; Brasier, 1995). Increasing nutrient input induces a decrease of carbonate production by reducing water transparency, (1) because of the increase of particular flux and (2) because these conditions favour the development of plankton at the top of the water column (Hallock and Schlager, 1986). This idea is supported by the presence of some foraminifers in the Guara limestones, like orbitolites or miliolids, that are associated with sea grass, which can develop under oligotrophic conditions and are replaced by algae when the conditions become eutrophic.

During the Bartonian, i.e. during the deposition of the deltaic sediments, few benthic foraminifers are observed and the fauna is mainly comprised of oysters and pectens, which are suspension-feeding organisms and echinoderms are abundantly represented too (Canudo et al., 1988; Millán et al., 1994; Castelltort et al., 2003). These species have specific ecologic preferences, and need large amounts of nutrients, contrary to shallow-water benthic foraminifers (Travé et al., 1996; Beavington-Penney and Racey, 2004). The increase of the detrital flux at the beginning of the Bartonian could then be invoked as the main factor forcing the disappearance of foraminifers by changing environmental conditions in the basin. Such conclusions were proposed

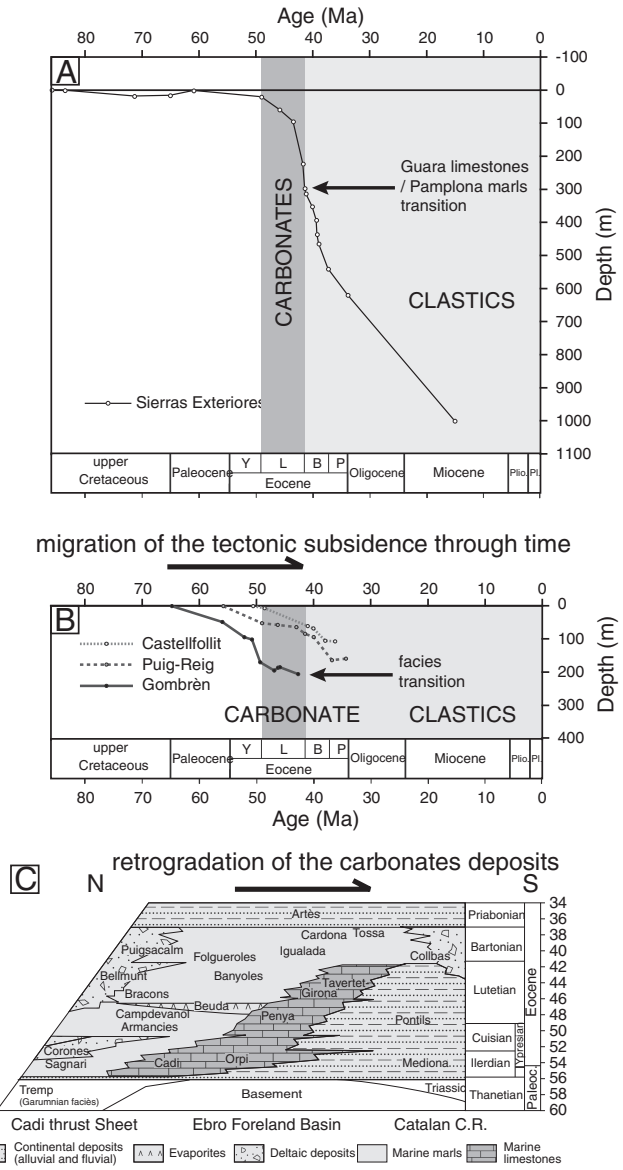

Fig. 13. (A) Evolution of the tectonic subsidence since the upper Cretaceous to the Miocene in the Sierras Exteriores along the Arguís section. (B) Evolution of the tectonic subsidence in the eastern part of the Ebro basin illustrating its migration to the south during the Eocene (modified after Vergés et al., 1998). (C) Evolution of the sedimentation in the eastern part of the Ebro basin during the Eocene illustrating the migration of the carbonate platforms to the south until the end of the Lutetian (modified after Vergés et al., 1998).

to explain the demise of the carbonate ramps in the French Alps by Sinclair et al. (1998) near the Eocene–Oligocene boundary. Both an increase of tectonic activity and a climatic switch to increased continental erosion rates can drive such a sedimentary pattern.

5.3. Basin tectonics

The transition from the Lutetian Guara carbonate ramp to the Bartonian deltaics (Arguís/Pamplona Marls) in the Jaca basin has been traditionally accounted by an increase of tectonic activity and the corresponding sudden deepening of the Jaca basin with a southward migration of the depocenter in response to the migration of the topographic load (Puigdefàbregas and Souquet, 1986; Barnolas and Teixell, 1994; Lafont, 1994; Millán et al., 1994; Payros et al., 1999), and the inferred associated arrival of increased terrigenous input.

Following the approach presented in Section 3.2, we have calculated the evolution of the tectonic subsidence along a profile following the Arguís section (Fig. 12). The obtained curve (Fig. 13a) shows a strong increase from ~0.3 m/Ma in the Mesozoic to ~25 m/Ma during the Lutetian, i.e. during deposition of the Guara Limestones, and to ~54 m/Ma during the Bartonian. Thus there is a significant increase in subsidence rate at the transition between the Guara Limestones and the Pamplona Marls (Fig. 13a). The subsidence then recedes slowly from the late Eocene to the Miocene. The strong increase observed in subsidence was already inferred by other authors (Puigdefàbregas and Souquet, 1986; Barnolas and Teixell, 1994; Lafont, 1994; Millán et al., 1994). The important change of sedimentation from carbonates to clastics correlates well at this particular location with the tectonic signal.

However, the deformation has propagated from east to west during the evolution of the Pyrenean orogeny and the loading and subsidence of the Iberian plate has followed this pattern continuously. The successive carbonate formations, usually representing carbonate ramps deposited on the southern border of the southern foreland, have kept up with this migration of the subsidence (Fig. 13b, c). For instance, in the eastern part of the southern foreland basin, Vergés et al. (1998) have documented the progressive migration of the tectonic subsidence from the north in the Paleocene to the south in the late Eocene (Fig. 13b). The Cadi, Orpi, Penya and Tavertet carbonate systems migrated from the north to the south with the migration of the subsidence, in the same fashion as the Boltaña and the Guara formations in the Jaca basin (Puigdefàbregas and Souquet, 1986). Therefore, we point out that the increased subsidence rates recorded here in the Jaca basin at the Lutetian–Bartonian transition are simply part of a continuous southward and westward progressive migration of the tectonic load in the South-Pyrenean foreland basin. In contrast to the previous history, the paleogeographic maps established above indicate that at the Lutetian–Bartonian boundary, the carbonate ramps disappeared synchronously at the scale of the entire South Pyrenean foreland.

5.4. Bartonian shift to high-frequency higher-amplitude sea level changes

Climate variations could have a strong influence on the continental erosion throughout sea-level variations. For example, in a study of the Eocene–Oligocene shift from carbonates to siliciclastics on the west African margin, Séranne (1999) proposed that a climate shift to cooler conditions and higher-amplitude, glacio-eustatically driven, sea-level changes was responsible for the demise of carbonate systems. In the Pyrenees, a simple field outlook at the Lutetian Guara carbonates and the Bartonian Belsué–Atarès deltaics suggests a contrast between a quiet and relatively monotonous carbonate deposition during the Lutetian versus marked high-frequency detrital cycles during the Bartonian. The identifiable cyclicities characteristic of each formation range in thickness from 1 to 8 m in the Lutetian carbonates to about 9 to 27 m in the Bartonian clastics (higher subsidence). According to the sedimentation rates of ~60 m/Ma in the Lutetian (Fig. 8) and ~250 m/Ma in the Bartonian (Castelltort et al., 2003) these thicknesses thus represent cyclicities of less than 100 ka.

We present here five detailed sections illustrating these high-frequency cycles in each of the Lutetian and Bartonian formations for which we quantify the possible amplitude of sea level variations. The estimated duration of each section, derived from the mean sedimentation rates, is reported on Fig. 14. We use the facies models established in this study and by Castelltort et al. (2003) for the carbonates and the deltaics respectively. The calculation of the accommodation is presented in Section 3.3.

Facies and paleobathymetries are more variable during deposition of the Bartonian deltaics. Depositional geometries and faunal associations indicate depositional paleoenvironments ranging from shoreface/intertidal deposition for the shallowest (5 ± 5 m) facies, to

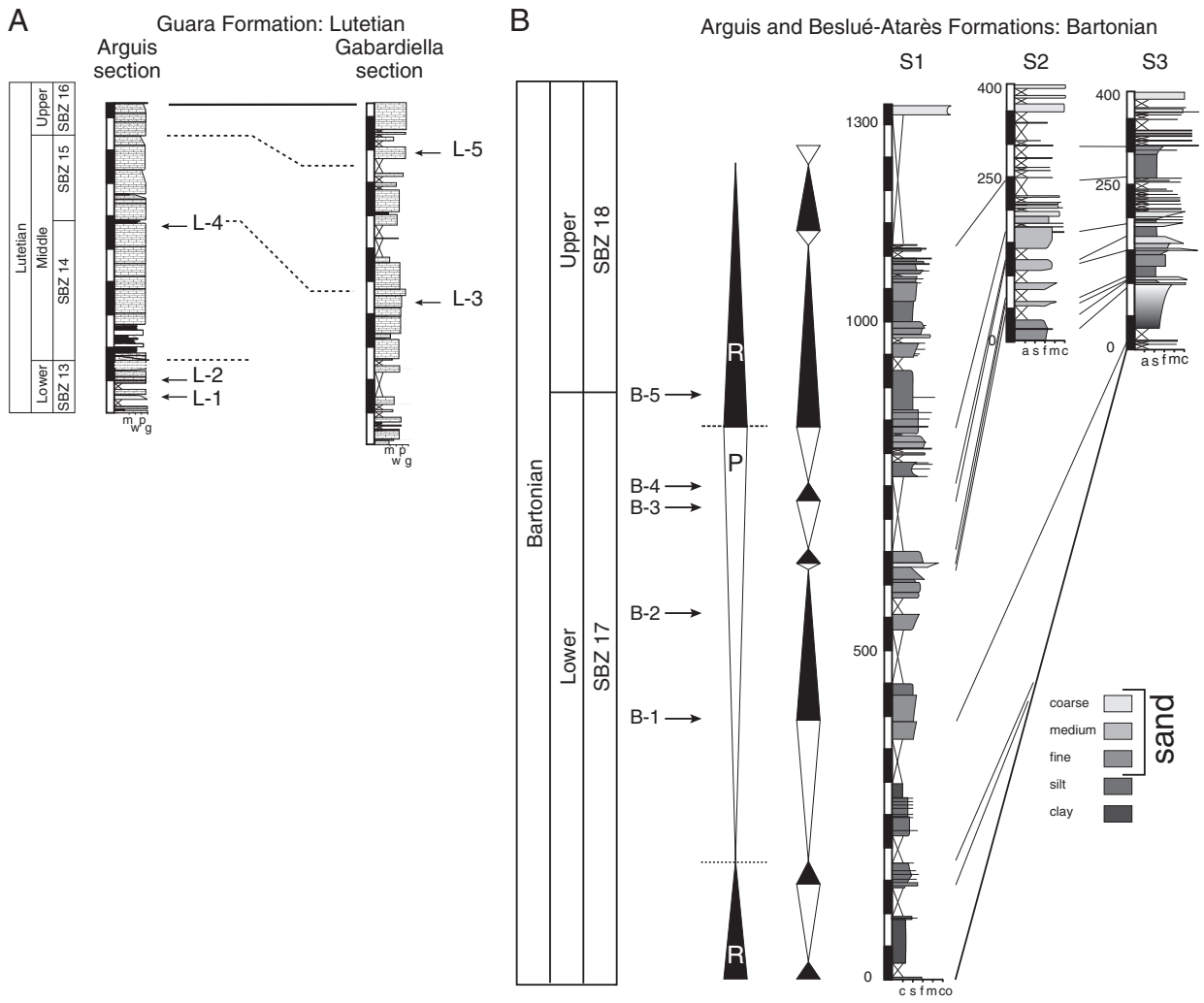

Fig. 14. Sedimentological successions of the Lutetian (A) (this study) and Bartonian series (B) (Castelltort et al., 2003). The Bartonian sedimentation is detrital with prodeltaic marls at the base and deltaic sandstones on the upper part. The 1300 m of section S1 were deposited during about 5 Ma (~250 m/Ma).

organic-rich marls with pro-delta turbidites for the deepest (100 ± m, cf Sztràkos and Castelltort, 2001; Castelltort et al., 2003). Calculated variations of accommodation during the Lutetian reveal amplitudes of variations from 5 m to 27 m for the sections L1 to L4 (Fig. 15, Table 3). L5 shows variations of 55 m, but its paleoenvironment corresponds to the outer ramp, where paleobathymetries uncertainties are higher than in the middle and inner ramp, i.e. for L1 to L4. Therefore, we can consider this elevated value to be an artefact.

Bartonian sediments exhibit more significant variations of accommodation, ranging from 25 to 55 m (Fig. 15, Table 4). Even if uncertainties may exist concerning the estimation of the paleobathymetries, cyclicities appear to be most contrasted during the Bartonian in comparison to the Lutetian, which is supported by the rapid changes of facies during this first period.

Relative sea level is the combination of vertical tectonic movements of the basement and absolute changes of sea-level (eustasy). Deformation is certainly responsible for the long-term background subsidence of the Jaca basin. However, to our knowledge there is no physical mechanism that explains cycles of tectonic uplift and subsidence responsible of ~20 m amplitude oscillations of the surface at the studied frequencies (<100 ka) (Miller et al., 2005).

During greenhouse periods, there seems to be no process able to remove significant quantities of water from the ocean and high-frequency sea level variations remain of limited amplitude of about 0.1 to 10 m (e.g., Rowley and Markwick, 1992; Schulz and Schäfer-Neth, 1997). In icehouse times, high-frequency cycles of water storage at the poles during glacials and its subsequent release during interglacials cause high-amplitude sea-level cycles often with Milankovitch periods or combinations (Hays et al., 1976). Within the limits of estimating the bathymetries of the facies observed in the Lutetian carbonates and the Bartonian clastics, the studied series exhibit a significant shift to higher amplitude relative sea-level cycles during the Bartonian. Thus, the relative sea-level cycles documented here may represent a record of the early establishment of glacio-eustasy.

6. Discussion: early signature of Cenozoic glaciations?

The sedimentary shift at the Lutetian–Bartonian from a carbonate to a deltaic sedimentary system can be correlated (Fig. 16) with (1) a shift to higher amplitude relative sea-level changes recorded in the same series, (2) a 25 m sea-level drop identified in the New Jersey and Delaware passive margins (Kominz et al., 2008) and east Tasman Plateau (Pekar et al., 2005), (3) an ~500 m lowering of the Pacific carbonate compensation depth (CCD; Tripati et al., 2005), and (4) an increase of $\delta^{18}O$ (Villa et al., 2008; Bohaty et al., 2009). All these events agree with a shift from greenhouse to partially icehouse conditions around the Lutetian–Bartonian boundary. Nevertheless, the precise timing for the observed shift is not exactly the same for the different signals. The deepening of sea-level in eastern America (Kominz et al., 2008) presents an acceleration during the beginning of the Bartonian,

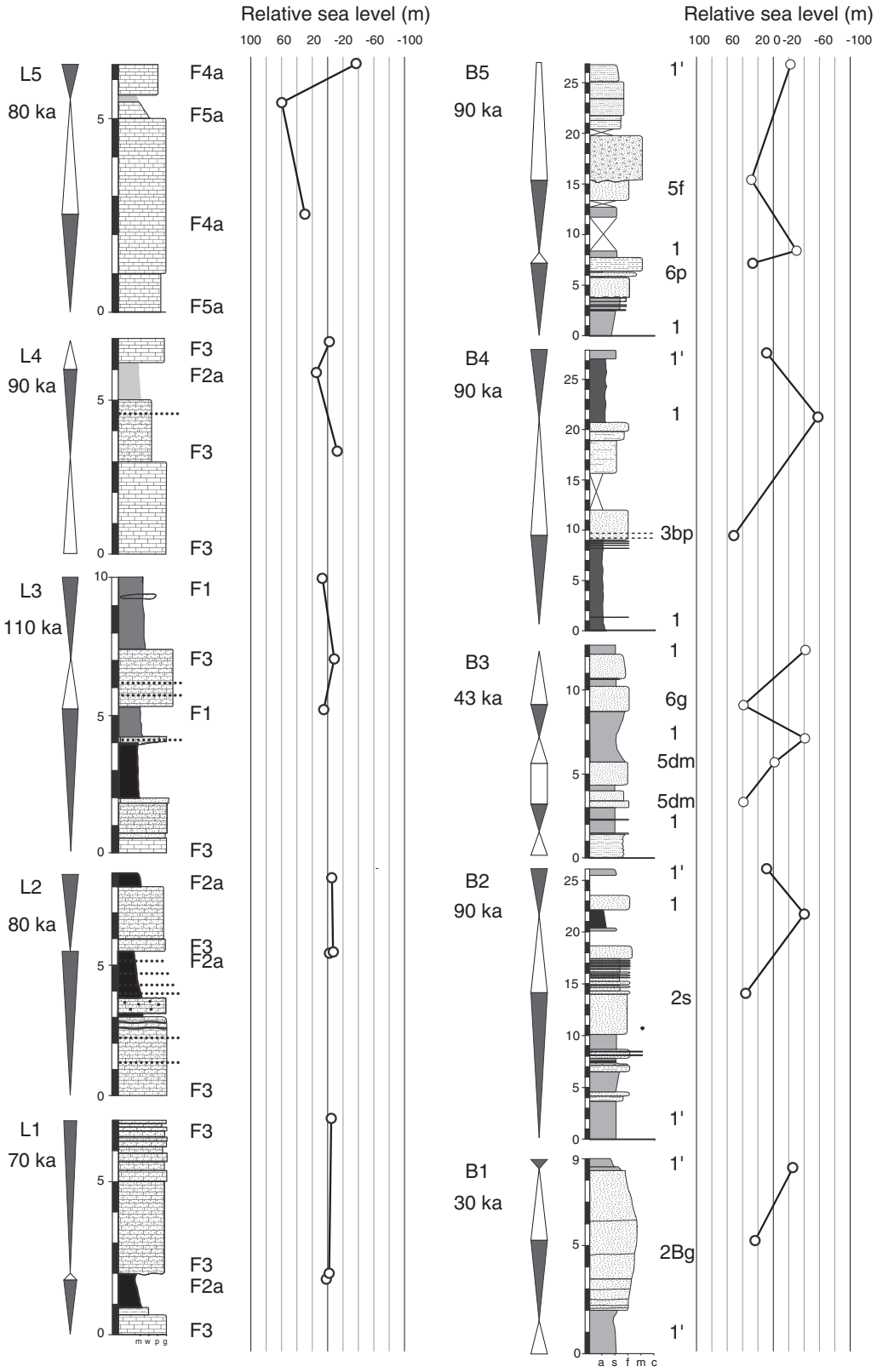

Fig. 15. Sedimentologic sections studied in the Lutetian (L1 to L5) and Bartonian (B1 to B5) sections. Geographic and stratigraphic locations of the sections are reported in Fig. 2 and Fig. 14 respectively. Variations of the accommodation have been calculated estimating paleobathymetries from facies models established in this study and Castelltort et al. (2003) for Lutetian and Bartonian sediments respectively (see attached Tables 1 and 2 for the correspondence between facies code and bathymetry).

whereas the deepening of the CCD (Tripati et al., 2005) happens closer to the Lutetian–Bartonian limit (Fig. 16). These two parameters should theoretically have the same and contemporaneous response to change in ice storage. However, these two curves were established in two different domains, i.e. in the western Atlantic and in the Pacific and dating methods were different in the two cases. We could reasonably conclude that the rapid deepening of the CCD and the sea-level reflect the same event.

Table 2
Data used to estimate the tectonic subsidence during the Mesozoic and the Cenozoic in the areas of Arguís. Age, thickness and paleobathymetries are from Millán (1996), Castelltort et al. (2003) and this study and refer to Fig. 12. Surface porosities, porosity-depth coefficients and sediment grain densities are from Allen and Allen (2005). Sea level variations are from Kominz et al. (2008).

Layer	Age	Depth	Thickness	Surface porosity	Porosity-depth coefficient	Sediment grain density	Sea-level	Paleo-bathymetry	Paleobathymetry uncertainty		Tectonic subsidence
	(Ma)	(m)	(m)		(km^{-1})	kg/m^3	(m)	(m)	(m)		(m)
1	85.8	3943	0	0.63	0.51	2720	54	0	0	0	0
2	83.5	3890	53	0.5	0.3	2710	74	20	−20	20	1.8
3	71.3	3852	38	0.5	0.3	2710	57	20	−20	20	19.4
4	65	3822	30	0.5	0.3	2710	57	10	−20	20	17.25
5	60.9	3742	80	0.533	0.345	2677	72	−20	−20	20	2.3
6	49	3742	0	0.533	0.345	2677	73	0	0	0	21.8
7	45.8	3662	80	0.512	0.318	2705	68	15	−15	15	55.1
8	43.6	3452	210	0.506	0.309	2707.5	79	0	−2	2	124.9
9	41.8	3322	130	0.506	0.309	2707.5	68	90	−30	30	133.9
10	41.46	3272	50	0.525	0.339	2706	65	150	−50	50	208.2
11	41.15	3245	27	0.548	0.372	2690	46	150	−50	50	314.1
12	40.03	3094	151	0.548	0.372	2690	50	150	−50	50	352.8
13	39.34	2647	447	0.547	0.369	2684	29	60	−30	30	393.6
14	39.22	2612	35	0.506	0.3	2669	22	90	−30	30	436.8
15	38.9	2522	90	0.602	0.462	2706	9	90	−30	30	465.8
16	37.24	2154	368	0.55	0.378	2702	55	90	−30	30	542.1
17	33.8	1600	554	0.49	0.27	2650	−11	−20	−20	50	621
18	15	0	1600	0.49	0.27	2650	−17	−100	−200	0	1001.3

As explained above, both climatic and tectonic changes could drive environmental stress for carbonate producers such as foraminifers with an excess of nutrient and lowering light intensity due to increasing erosion and sediment supply (Hallock and Schlager, 1986). However, we have shown that the timing of the local tectonic disturbance was part of a continuum of westward and southward development of the Pyrenean orogen, whereas the shift from the last carbonate platforms to clastic sediments was synchronous at the scale of the whole basin.

Considering the correlations between the sedimentary trend and the climatic evolution of the middle Eocene (Fig. 16), we propose that it is such a climatic shift that is responsible for the increase of sediment supply in the South-Pyrenean basin and thus, the demise of Eocene carbonates in the Pyrenees. However, Vergés et al. (1995) have shown that since the middle Lutetian, the topography raised progressively in the eastern part of the Pyrenees at the same time as rates of shortening decreased in the same area. Moreover, extensive carbonate systems subsisted in other foreland basins, like in the French Alps, after the Lutetian–Bartonian limit even though they were mostly made of the same carbonate producers as the Pyrenean Lutetian carbonate formations, i.e. shallow-water benthic foraminifers (Sinclair, 1997; Sinclair et al., 1998). Therefore, the sedimentary transition cannot be a simple consequence of the transient cooling around the Lutetian–Bartonian boundary only. Indeed, it is likely that the increase in detrital sedimentary flux in the eastern Pyrenees since the middle Lutetian is the consequence of the rise of the Pyrenean topography because it occurred before the climatic shift. Moreover, this trend corresponds to the transition from underfilled to overfilled state in this area of the foreland basin, traditionally explained by the tectonically driven lateral growth of the orogen (Sinclair, 1997).

Table 3
Data used to calculate accommodation for the Lutetian detail sections (Fig. 15). Facies codes, environments, ages and thickness are from Millán (1996), Castelltort et al. (2003) and this study and refer to Fig. 14. Surface porosities, porosity-depth coefficients and sediment grain densities are from Allen and Allen (2005). Sea level variations are from Kominz et al. (2008).

	Surface	Facies code	Environment	Age	Depth	Surface porosity	Porosity-depth coefficient	Sediment grain density	Sea-level	Paleo-bathymetry	Paleo-bathymetry uncertainty		Accommodation variation
				(Ma)	(m)		(km^{-1})	(kg/m^3)	(m)	(m)	(m)		(m)
L1	MFS1	F3	Inner ramp	47.6	3722	0.252	0.204	1088	68	7.5	7.5	7.5	
	FS1	F2a	Lagoon		3720.2	0.35	0.258	1618	68	5	10	10	−3.5
	MFS2	F3	Inner ramp		3720	0.161	0.105	802	68	7.5	7.5	7.5	5.3
	FS2	F3	Inner ramp		3715	0.161	0.105	802	68	5	5	5	2.7
L2	MFS1	F3	Inner ramp	47.25	3692	0.21	0.132	1067	58	7.5	7.5	7.5	
	FS1	F2a	Lagoon		3686.5	0.21	0.132	1067	58	5	10	10	−2.1
	MFS2	F3	Inner ramp		3681	0.21	0.132	1067	58	7.5	7.5	7.5	15.4
	FS2	F2a	Lagoon		3672.5	0.21	0.132	1067	58	5	10	10	−1.7
L3	MFS1	F3	Inner ramp	44.5	3532	0.574	0.414	2692	81	7.5	7.5	7.5	
	FS1	F1	Shoreline		3527	0.413	0.309	1890	81	0	5	5	−12
	MFS2	F3	Inner ramp		3525	0.196	0.108	1060	81	7.5	7.5	7.5	6.7
	FS2	F1	Shoreline		3522	0.5845	0.4605	2577	81	0	5	5	−3.4
L4	FS1	F3	Inner ramp	43.65	3467	0.513	0.321	2711	45	7.5	7.5	7.5	
	MFS1	F3	Inner ramp		3464.5	0.513	0.321	2711	45	20	30	30	5.6
	FS2	F2a	Lagoon		3461.5	0.537	0.357	2701	45	5	10	10	−14.2
	MFS2	F3	Inner ramp		3460.5	0.513	0.321	2711	45	7.5	7.5	7.5	5.3
L5	MFS1	F5a	Outer ramp	42.3	3342	0.513	0.321	2711	65	90	30	30	
	FS1	F5a	Outer ramp		3338.8	0.513	0.321	2711	65	60	10	10	−24.2
	MFS2	F5a	Outer ramp		3336	0.526	0.342	2712	65	90	30	30	30.7
	FS2	F4a	Middle ramp		3335	0.513	0.321	2711	65	37.5	22.5	22.5	−29.7

Table 4
Data used to calculate accommodation for the Bartonian detail sections (Fig. 15). Facies codes, paleo-environments, and paleo-water depths are from Castelltort et al. (2003) and refer to Fig. 14. Surface porosities, porosity-depth coefficients and sediment grain densities are from Allen and Allen (2005). Sea level variations are from Kominz et al. (2008).

	Surface	Facies code	Environment	Age	Depth	Surface porosity	Porosity-depth coefficient	Sediment grain density	Sea-level	Paleo-bathymetry	Paleo-bathymetry uncertainty		Accommodation variation
				(Ma)	(m)		(km^{-1})	(kg/m^3)	(m)	(m)	(m)		(m)
B1	MFS1	1′	Lower to distal upper offshore silty shelf	39.85	2890	0.56	0.39	2685	50	75	25	25	
	FS1	2Bg	Upper offshore prodelta/distal delta front		2886.5	0.532	0.342	2671	50	50	20	20	−24
	MFS2	1′	Lower to distal upper offshore silty shelf		2883.2	0.518	0.318	2664	50	75	25	25	26
B2	MFS1	1	Lower offshore silty shelf	39.4	2700	0.56	0.39	2685	29	60	30	30	
	FS1	2 s	Upper offshore prodelta		2685.5	0.504	0.294	2657	29	20	10	10	−35.6
	MFS2	1	Lower offshore silty shelf		2678	0.616	0.486	2713	29	60	30	30	41.6
	FS2	1′	Lower to distal upper offshore silty shelf		2674	0.602	0.462	2706	29	50	30	30	−9
B3	MFS1	1	Lower offshore silty shelf	39.1	2580	0.532	0.342	2671	22	60	30	30	
	FS1	5 dm	Proximal upper offshore		2578.3	0.56	0.39	2685	22	20	10	10	−39.5
	FS1′	5 dm			2575.8	0.518	0.318	2664	22	20	10	10	0.7
	MFS2	1	Lower offshore silty shelf		2574.3	0.518	0.318	2664	22	60	30	30	40.4
	FS2	6 g	Upper offshore proximal ramp		2572.2	0.546	0.366	2678	22	20	10	10	−39.4
	MFS3	1	Lower offshore silty shelf		2569	0.518	0.318	2664	22	60	30	30	40.9
B4	MFS1	1	Lower offshore silty shelf	38.8	2510	0.616	0.486	2713	9	60	30	30	
	FS1	3 bp	Upper offshore to lower shoreface/bypass in deltafront environment		2500.5	0.504	0.294	2657	9	5	5	5	−51.9
	MFS2	1	Lower offshore silty shelf		2489.5	0.518	0.318	2664	9	60	30	30	58.1
	FS2	1′	Lower to distal upper offshore silty shelf		2483	0.602	0.462	2706	9	50	30	30	−8.5
B5	MFS1	1	Lower offshore silty shelf	38.5	2420	0.574	0.414	2692	8	60	30	30	
	FS1	6p	Upper offshore median ramp		2415.7	0.518	0.318	2664	8	30	10	10	−28.7
	MFS2	1	Lower offshore silty shelf		2415.1	0.546	0.366	2678	8	60	30	90	30.2
	FS2	5f	Distal upper offshore		2404.3	0.518	0.318	2664	8	30	30	30	−26.9
	MFS3	1′	Lower to distal upper offshore silty shelf		2393	0.532	0.342	2671	8	50	30	30	23.1

Because carbonate platforms have subsisted until the end of the Lutetian all around the Pyrenees despite the east–west diachronous increase of the tectonic activity and associated increased supply of detrital sediments, it appears that this tectonic trend alone was not sufficient to provoke the drowning and demise of carbonates. Similarly, changing climatic conditions were also not sufficient alone to cause the demise of the carbonates, because well expressed carbonate platforms persisted after the Lutetian in the Alps. We thus propose that the demise of the carbonate platforms in the Pyrenees may rather be the result of the combination of several factors and in particular a climatic instability combined to the existence of a significant topography to supply detrital material (Vergés et al., 1995). In this vision, tectonics and climate should have both exerted an influence on the end of the carbonate platforms, but at different time scales. The

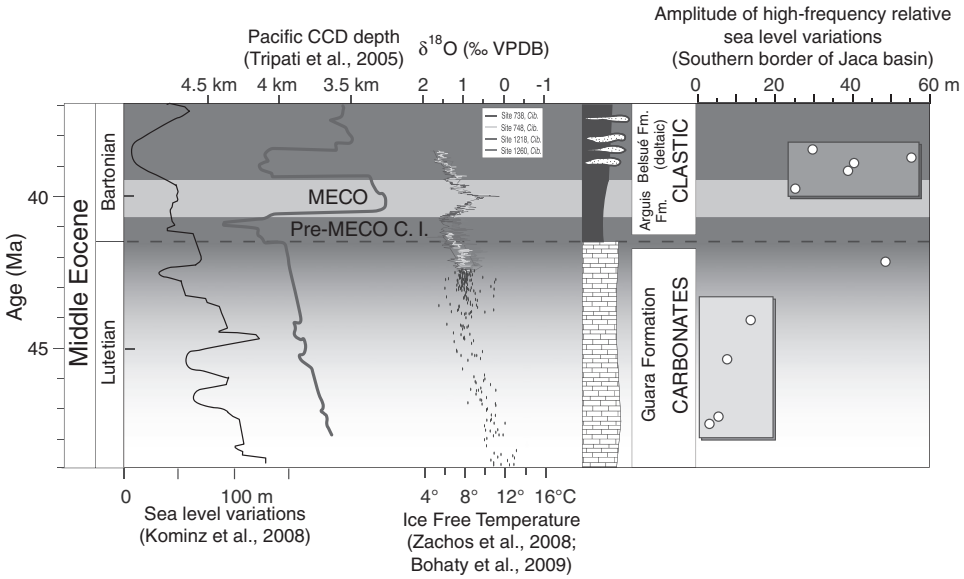

Fig. 16. Simplified evolution of the sedimentation during the middle Eocene correlated with the evolution of high frequency sea-level variations, the long-term sea level variations (Kominz et al., 2008), the evolution of the carbonate compensation depth in the Pacific (Tripati et al., 2005) and the deep-sea $\delta^{18}O$ and temperatures (points correspond to Zachos et al., 2008; lines correspond to Bohaty et al., 2009). MECO means Middle Eocene Climatic Optimum and Pre-MECO C.I. means Pre Middle Eocene Climatic Optimum Cooling Interval.

continuous increase of the paleotopography played a continuous and progressive influence on the drowning of the platforms by increasing the subsidence since the beginning of the Eocene (Fig. 13), while the change in climate played a more instantaneous role. In this view, tectonics prepared the ground for a drowning of the platforms and climate change was responsible for their definitive death.

Climate change and increase of erosion are not simply related factors. In the case of the middle Eocene, the process seems to be related to the shift from icehouse to greenhouse conditions. Indeed, during greenhouse periods, climatic conditions are stable and erosion in an orogenic domain may be primarily limited by uplift. On the contrary, during icehouse intervals, sea-level is influenced by the waning and waxing of continental ice-sheets in response to orbital forcing (Hays et al., 1976). As a consequence, the magnitude of sea level variations is likely to be more important than during greenhouse periods, potentially inducing greater erosion on the continents (Fisk, 1944; Knox, 1983; Posamentier and Vail, 1988; Miller et al., 1991; Séranne, 1999). Rivers continuously need to adjust their bed to a new equilibrium profile attached to sea-level and this creates frequent rejuvenation of the drainage basins. This may therefore favour erosion and the detrital material supply to the basins may increase with respect to greenhouse periods.

The influence of high-frequency sea-level cycles on river systems is however not a trivial problem. It can be postulated that base level change has a greater effect on river systems when their gradient is low. Therefore, as opposed to the French Alps, the Pyrenean foreland basin was already in its filled stage east of the Jaca basin at the Lutetian–Bartonian boundary, with extensively developed low gradient alluvial systems (Escanilla Formation, Capella Formation and Cajigar Formation; Vincent, 2001; Beamud et al., 2003). These low gradient alluvial plains may have reacted strongly to high-frequency cycles of sea-level changes as compared to high-gradient transverse systems draining the axial zone in the Pyrenees or the Alps. This is probably why the global climatic event that happened near the Lutetian–Bartonian limit had a geographic impact on the erosion and the sedimentation limited to the Pyrenees, and did not affect significantly the Alps, which were not enough elevated. Thus, the release of significant amounts of fine material from these foreland alluvial plains because of higher amplitude sea-level variations should have been responsible for changing environmental conditions in the shallow marine realm of the foreland basin and induced the disappearance of the carbonates.

This study shows that the example of the South-Pyrenean foreland basin does not follow a classical tectonostratigraphic evolution. Previous works that were interested in the causes of the demise of the carbonate platforms of the alpine foreland basin (Crampton and Allen, 1995; Sinclair, 1997; Allen et al., 2001) all pointed the tectonics as the main driver. In particular, Allen et al. (2001) successfully reproduced the growth of the Eocene alpine carbonate ramps and showed that their drowning primarily resulted from the variation of environmental parameters (light extinction coefficient) and tectonic parameters such as the flexural rigidity and convergence rate. The case of the Pyrenean system documents a different scenario in which the demise of the carbonate platforms is the consequence of a superimposition of climate change over enhanced deformation.

7. Conclusion

The study of the six sections presented in this work demonstrates that the Guara Limestone Formation was deposited during the whole Lutetian in the Sierras Exteriores, i.e. from SBZ 13 to SBZ 16. These limestones are mainly composed of shallow-water benthic foraminifers, and were deposited from inner ramp to outer ramp environment. The sedimentation was perturbed during the upper Lutetian by the growth of the Pico del Aguila and Gabardiella anticlines, which forced the distribution of the facies, but not the nature of the sedimentation, i.e. carbonates or siliciclastics. Secondly, we demonstrate that a major sedimentation change happened at the scale of the South-Pyrenean foreland basin at the Lutetian–Bartonian boundary (~41.3 Ma) with the definitive disappearance of marine carbonate platforms. The tectonic subsidence increases in the Jaca basin across this boundary, but we point out that this local increase is part of a continuum of migration of the subsidence at the scale of the South-Pyrenean foreland basin as already suggested by others. Previously, the Pyrenean carbonate ramps and platforms adapted to this migration, whereas they disappeared regionally at the Lutetian–Bartonian boundary. The high-frequency relative sea-level variations derived from small-scale field sections however show a pronounced shift to higher amplitude relative sea-level changes in the Bartonian. With these observations and considering the known global cooling recorded in the Pacific CCD, global sea-level and carbonates $\delta^{18}O$, we are lead to propose that the Pyrenean carbonates were early victims of the progressive shift to icehouse conditions that started in the Cenozoic. The precise localisation of this phenomenon in the active collisional Pyrenees however suggests that it is the destabilization of established rivers and the ensuing increased erosion and sediment flux to the basin that determined the extinction of Pyrenean ramps rather than a direct global climatic impact on the carbonates such as temperature or episodic exposure due to sea-level changes. Harsher climates superimposed on intense tectonics seem to have constituted a deadly combination for the Pyrenean foreland carbonates.

Acknowledgements

This study was funded by a PhD grant from the French Ministry of Research and Education to Damien Huyghe and by funds from UPMC and CNRS to UMR 7072 (now UMR 7193) and JE-2477. Castelltort acknowledges Willett's ESD funds for support. We would like to thank two anonymous reviewers and editor G.J. Weltje for their constructive comments. Many thanks to Matthew Fox at ETH for improving the English. We warmly thank the friendly crews at Roda de Isabena, Nocito and Arguís.

References

Agustí, J., Pérez-Rivarés, F.J., Cabrera, L., Garcés, M., Pardo, G., Arenas, C., 2011. The Ramblian–Aragonian boundary and its significance for the European Neogene continental chronology. Contributions from the Ebro Basin record (NE Spain). Geobios 44, 121–134.

Allen, P.A., Allen, J.R., 2005. Basin Analysis: Principles and Applications, second edition. Blackwell Publishing. (560 p.).

Allen, P.A., Burgess, P.M., Galewsky, J., Sinclair, H.D., 2001. Flexural–eustatic numerical model for drowning of the Eocene perialpine carbonate ramp and implications for Alpine geodynamics. Geological Society of America Bulletin 113, 1053–1066.

Barnolas, A., Teixell, A., 1994. Platform sedimentation and collapse in a carbonate-dominated margin of a foreland basin (Jaca basin, Eocene, southern Pyrenees). Geology 22, 1107–1110.

Beamud, E., Garcés, M., Cabrera, L., Muñoz, J.A., Almar, Y., 2003. A new middle to late Eocene continental chronostratigraphy from NE Spain. Earth and Planetary Science Letters 216, 501–514.

Beavington-Penney, S., Racey, A., 2004. Ecology of extant nummulitids and other larger benthic foraminifera: applications in palaeoenvironmental analysis. Earth Sciences Reviews 67, 219–265.

Bentham, P.A., Burbank, D.W., 1996. Chronology of Eocene foreland basin evolution along the western oblique margin of the South-Central Pyrenees. In: Friend, P.F., Dabrio, C.J. (Eds.), Tertiary Basins of Spain. : World and Regional Geology, E11. Cambridge University Press, pp. 144–152.

Bentham, P.A., Burbank, D.W., Puigdefàbregas, C., 1992. Temporal and spatial controls on the alluvial architecture of an axial drainage system: late Eocene Escanilla Formation, southern Pyrenean foreland basin, Spain. Basin Research 4, 335–352.

Berggren, W.A., Kent, D.V., Swisher, C.C., Aubry, M.P., 1995. A revisited Cenozoic geochronology and chronostratigraphy. In: Berggren, W.A., Kent, D.V., Aubry, M.P., Hardenbol, J. (Eds.), Geochronology, Time Scales and Global Stratigraphic Correlations: SEPM Special Publication 54, pp. 129–212.

Bohaty, S.M., Zachos, J.C., Florindo, F., Delaney, M.L., 2009. Coupled greenhouse warming and deep-sea acidification in the middle Eocene. Paleoceanography 24. doi:10.1029/2008PA001676.

Bosence, D., 2005. A genetic classification of carbonate platforms based on their basinal and tectonic settings in the Cenozoic. Sedimentary Geology 175, 49–72.

Brasier, M.D., 1975. An outline history of seagrass communities. Palaeontology 18, 681–702.
Brasier, M.D., 1995. Fossils indicators of nutrient levels. 2: Evolution and extinction in relation to oligotrophy. In: Bosence, D.W.J., Allison, P.A. (Eds.), Marine Palaeoenvironmental Analysis from Fossils: Geological Society Special Publication, 83, pp. 133–150.
Burbank, D.W., Puigdefàbregas, C., Muñoz, J.A., 1992. The chronology of the Eocene tectonic and stratigraphic development of the eastern Pyrenean Foreland Basin, NE Spain. Geological Society of America Bulletin 104, 1101–1120.
Burchette, T.P., Wright, V.P., 1992. Carbonate ramp depositional systems. Sedimentary Geology 79, 3–57.
Butts, S.H., 2005. Latest Chesterian (Carboniferous) initiation of Gondwanan glaciation recorded in facies stacking patterns and brachiopod paleocommunities of the Antler foreland basin, Idaho. Palaeogeography, Palaeoclimatology, Palaeoecology 223, 275–289.
Caja, M.A., Marfil, R., Garcia, D., Remacha, E., Morad, S., Mansurberg, H., Amorosi, A., Martinez-Calvo, C., Lahoz-Beltra, R., 2010. Provenance of siliciclastic and hybrid turditic arenites of the Eocene Hecho Group, Spanish Pyrenees: implications for the tectonic evolution of a foreland basin. Basin Research 22, 157–180.
Canudo, J.-I., Molina, E., Riveline, J., Serra-Kiel, J., Sucunza, M., 1988. Les évènements biostratigraphiques de la zone prépyrénéenne d'Aragon (Espagne), de l'Eocène Moyen à l'Oligocène Inférieur. Revue de Micropaleontologie 31, 15–29.
Castelltort, S., Guillocheau, F., Robin, C., Rouby, D., Nalpas, T., Lafont, F., Eschard, R., 2003. Fold control on the stratigraphic record: a quantified sequence stratigraphic study of the Pico del Aguila anticline in the south-western Pyrenees (Spain). Basin Research 15, 527–551.
Caus, E., Serra-Kiel, J., 1992. Macroforaminifers: Estructura, Paleoecologia I Bioestratigrafia. Publicaciò del Servei Geològic de Catalunya. : Monografia 2, Barcelona, Spain..
Crampton, S.L., Allen, P.A., 1995. Recognition of forebulge unconformities associated with early stage foreland basin development: example from the North Alpine foreland basin. AAPG Bulletin 79, 1495–1514.
DeCelles, P.G., Giles, K.N., 1996. Foreland basin systems. Basin Research 8, 105–123.
Dercourt, J., Zonenshain, L.P., Ricou, L.E., Kazmin, V.G., Le Pichon, X., Knipper, A.L., Grandjacquet, C., Sborshchikov, I.M., Geyssant, J., Lepvrier, C., Pechersky, D.H., Boulin, J., Sibuet, J.C., Savostin, L.A., Sorokhtin, O., Westphal, M., Bazhenov, M.L., Lauer, J.P., Biju-Duval, B., 1986. Geological evolution of the Tethys Belt from the Atlantic to the Pamirs since the Lias. In: Aubouin, J., Le Pichon, X., Monin, A.S. (Eds.), Evolution of the Tethys: Tectonophysics, 123, pp. 241–315.
Dorobek, S., 1995. Synorogenic carbonate platforms and reefs in foreland basins: controls on stratigraphic evolution and platform/reef morphology. In: Dorobek, S., Ross, G.M. (Eds.), Stratigraphic Evolution of Foreland Basins: SEPM Special Publication, pp. 583–594.
Dreyer, T., 1993. Quantified fluvial architecture in ephemeral stream deposits of the Esplugafreda Formation (Paleocene), Tremp–Graus Basin, northern Spain. Special Publication International Association Sedimentology 17, 337–362.
Dreyer, T., Corregidor, J., Arbues, P., Puigdefàbregas, C., 1999. Architecture of the tectonically influenced Sobrarbe deltaic complex in the Ainsa basin, northern Spain. Sedimentary Geology 127, 127–169.
Fisk, H.N., 1944. Geological Investigation of the Alluvial Valley of the Lower Mississippi River. Mississippi River Commission, Vicksburg.
Geel, T., 2000. Recognition of stratigraphic sequences in carbonate platform and slope deposits: empirical models based on microfacies analysis of Palaeogene deposits in southeastern Spain. Palaeogeography, Palaeoclimatology, Palaeoecology 155, 211–238.
Hallock, P., Schlager, W., 1986. Nutrient excess and the demise of coral reefs and carbonate platforms. Palaios 1, 389–398.
Hay, W.W., Sloan, J.L., Wold, C.N., 1988. Mass/age distribution and composition of sediments on the ocean floor and the global rate of sediment subduction. Journal of Geophysical Research 93 (B12), 14933–14940.
Hays, J.D., Imbrie, J., Shackleton, N.J., 1976. Variations in the Earth's orbit: pacemaker of the Ice Ages. Science 194, 1121–1132.
Hogan, P.J., Burbank, D.W., 1996. Evolution of the Jaca piggyback basin and emergence of the External Sierras, southern Pyrenees. In: Friend, P.F., Dabrio, C.J. (Eds.), Tertiary Basins of Spain. Cambridge Univ. Press, pp. 153–160.
Hottinger, L., 1960. Uber paleocaene und eocaene Alveolinen. Eclogae Geologicae Helvetiae 53, 265–283.
Hottinger, L., 1983. Processes determining the distribution of larger foraminifera in space and time. Utrecht Micropaleontological Bulletin 30, 239–253.
Hottinger, L., 1997. Shallow benthic foraminiferal assemblages as signals for depth of their deposition and their limitations. Bulletin de la Société Géologique de France 168, 491–505.
Hottinger, L., Drobne, K., 1988. Alvéolines tertiaires: Quelques problèmes liés à la conception de l'espèce. Revue de Paléobiologie 2, 665–685.
Huyghe, D., Mouthereau, F., Castelltort, S., Filleaudeau, P.-Y., Emmanuel, L., 2009. Paleogene propagation of the southern Pyrenean thrust wedge revealed by finite strain analysis in frontal thrust sheets: implications for mountain building. Earth and Planetary Science Letters 288, 421–433.
Jervey, M.T., 1988. Quantitative geological modeling of siliclastic rock sequences and their seismic expressions. In: Wilgus, C.K., et al. (Ed.), Sea-level Changes: An Integrated Approach: Society of Economic Paleontologists and Mineralogists Special Publication, 42, pp. 47–69.
José, D., Rios, M., Almela, D.A., 1951. Mapa geologico de Apiès, 1/50 000. Institu Geologico y Miniero de España.
Knox, J.C., 1983. Responses of river systems to Holocene climates. In: Wright, H.E., Porter, S.C. (Eds.), Late Quaternary Environments of the United States, 2, the Holocene. University of Minnesota Press, pp. 26–41.
Kominz, M.A., Browning, J.V., Miller, K.G., Sugarman, P.J., Mizintsevat, S., Scotese, C.R., 2008. Late Cretaceous to Miocene sea-level estimates from the New Jersey and Delaware coastal coreholes: an error analysis. Basin Research 20, 211–226.
Lafont, F., 1994. Influences relatives de la subsidence et de l'eustatisme sur la localisation et la géometrie des reservoirs d'un système deltaique. Exemple de l'Eocene du bassin de Jaca (Pyrenees espagnoles). PhD Thesis, University of Rennes, France, 264 pp.
Lanaja, J.M., 1987. Contribución de la Exploración Petrolífera al conocimiento de la geología de España. Publ. IGME, Madrid. (465p.).
Lear, C.H., Elderfield, H., Wilson, P.A., 2000. Cenozoic deep-sea temperatures and global ice volumes from Mg/Ca in benthic foraminiferal calcite. Science 287, 269–272.
Leutenegger, S., 1984. Symbiosis in benthic foraminifera: specificity and host adaptations. Journal of Foraminiferal Research 14, 16–35.
Lopez-Blanco, M., 2002. Sedimentary response to thrusting and fold growing on the SE margin of the Ebro basin (Paleogene, NE Spain). Sedimentary Geology 146, 133–154.
Losantos, M., Aragonès, E., Berastegui, X., Palau, J., Puigdefàbregas, C., 1989. Institut cartografic de Catalunya, 1989. Mapa geologic de Catalunya, 1/250 000. Servei geologic de Catalunya, Barcelona.
Luterbacher, H., 1998. Sequence stratigraphy and the limitations of biostratigraphy in the marine Paleogene strata of the Tremp Basin (central part of the southern Pyrenean foreland basin, Spain). In: De Graciansky, P.C., Hardenbol, J., Jacquin, T., Vail, P.R. (Eds.), Mesozoic and Cenozoic Sequence Stratigraphy of European Basins: Society for Sedimentary Geology Special Publication, 60, pp. 303–309.
Millán, H., 1996. Estructura y cinematica del frente de cabalgamiento surpirenaico, Sierras Exteriores aragonesas, PhD Thesis, Universidad de Zaragoza, Spain, 330 pp.
Millán, H., Aurell, M., Meléndez, A., 1994. Synchronous detachment folds and coeval sedimentation in the Prepyrenean External Sierras (Spain): a case study for a tectonic origin of sequences and systems tracts. Sedimentology 41, 1001–1024.
Millán, H., Den Bezemer, T., Vergés, J., Marzo, M., Muñoz, J.A., Roca, E., Cirès, J., Zoetemeijer, R., Cloetingh, S., Puigdefàbregas, C., 1995. Paleo-elevation and EET evolution at mountain ranges: inferences from flexural modelling in the Eastern Pyrenees and Ebro Basin. Marine and Petroleum Geology 12, 917–928.
Miller, K.G., Fairbanks, R.A., Mountain, G.S., 1987. Tertiary oxygen isotope synthesis, sea- level history and continental margin erosion. Paleoceanography 2, 1–19.
Miller, K.G., Wright, J.D., Fairbanks, R.G., 1991. Unlocking the Ice House: Oligocene–Miocene oxygen isotopes, and margin erosion. Journal of Geophysical Research 96 (B4), 6829–6848.
Miller, K.G., Kominz, M.A., Browning, J.V., Wright, J.D., Mountain, G.S., Katz, M.E., Sugarman, P.J., Cramer, B.S., Christie-Blick, N., Pekar, S.F., 2005. The Phanerozoic record of global sea-level change. Science 310, 1293–1298.
Molina, E., Ortiz, N., Serra-Kiel, J., 1988. Implicationes paleoecologicas de los foraminiferos en el Eocene del Prepirineo oscense (sector de Arguís). Revista Espanola de Paleontologia 3, 45–57.
Molnar, P., England, P., 1990. Late Cenozoic uplift of mountain ranges and global climate change: chicken or egg? Nature 346, 29–34.
Muñoz, J.A.E., 1992. Evolution of a continental collision belt: ECORS-Pyrenees crustal balanced cross-section. In: McClay, K. (Ed.), Thrust Tectonics. Chapman & Hall, pp. 235–246.
Muñoz, J.A., Martinez, A., Vergés, J., 1986. Thrust sequences in the eastern Spanish Pyrenees. Journal of Structural Geology 8, 399–405.
Mutti, E., 1977. Distinctive thin-bedded turbidite facies and related depositional environments in the Eocene Hecho Group (South-central Pyrenees, Spain). Sedimentology 24, 107–131.
Nijman, W., 1998. Cyclicity and basin axis shift in a piggyback basin: towards modelling of the Eocene Tremp-Ager Basin, South Pyrenees, Spain. In: Mascle, A., Puigdefàbregas, C., Luterbacher, H.P., Fernandez, M. (Eds.), Cenozoic Foreland Basins of Western Europe: Geological Society Special Publications, 134, pp. 135–162.
Pagani, M., Zachos, J.C., Freeman, K.H., Tipple, B., Bohaty, S., 2005. Marked decline in atmospheric carbon dioxide concentrations during the Paleogene. Science 309, 600–603.
Payros, A., 1997. El Eoceno de la Cuenca de Pamplona : estratigrafia, facies y evolucion paleogeographica. PhD Thesis, University Basque Country, Bilbao, Spain, 403 pp.
Payros, A., Pujalte, V., Orue-Etxebarria, X., 1999. The South Pyrenean Eocene carbonate megabreccias revisited: new interpretation based on evidence from the Pamplona Basin. Sedimentary Geology 125, 165–194.
Pearson, P.N., Palmer, M.R., 2000. Atmospheric carbon dioxide concentration over the past 60 million years. Nature 406, 695–699.
Pearson, P.N., Foster, G.L., Wade, B.S., 2009. Atmospheric carbon dioxide through the Eocene–Oligocene climate transition. Nature 461, 1110–1113.
Peizhen, Z., Molnar, P., Downs, W.R., 2001. Increase sedimentation rates and grain sizes 2–4 Myr ago due to the influence of climate change on erosion rates. Nature 410, 891–897.
Pekar, S.F., Hucks, A., Fuller, M., Li, S., 2005. Glacioeustatic changes in the early and middle Eocene (51–42 Ma): shallow-water stratigraphy from ODP Leg 189 Site 1171 (South Tasman Rise) and deep-sea $\delta^{18}O$ records. Geological Society of America Bulletin 117, 1081–1093. doi:10.1130/B25486.1.
Plaziat, J.-C., 1981. Late Cretaceous to Late Eocene palaeogeographic evolution of southwest Europe. Palaeogeography, Palaeoclimatology, Palaeoecology 36, 263–320.
Posamentier, H.W., Vail, P.R., 1988. Eustatic controls on clastic deposition II — sequence and systems tract models. In: Wilgus, C., Hastings, B., Ross, C., Posamentier, H., Van Wagoner, J., Kendall, C. (Eds.), Sea-Level Changes : An Integrated Approach: Society of Economic Paleontologists and Mineralogists Special Publication, 42, pp. 47–69 (Tulsa).

Pueyo, E.L., Millán, H., Pocoví, A., 2002. Rotation velocity of a thrust: a paleomagnetic study in the External Sierras (Southern Pyrenees). Sedimentary Geology 146, 191–208.
Puigdefàbregas, C., 1975. La sedimentación molásica en la cuenca de Jaca. Pirineos 104, 1–188.
Puigdefàbregas, C., Souquet, P., 1986. Tecto-sedimentary cycles and depositional sequences of the Mesozoic and Tertiary from the Pyrenees. Tectonophysics 129, 173–203.
Puigdefàbregas, C., Muñoz, J.A., Vergés, J., 1992. Thrusting and foreland basin evolution in the southern Pyrenees. In: McClay, K. (Ed.), Thrust Tectonics. Chapman & Hall, London, pp. 247–254.
Pujalte, V., Baceta, J.I., Schmitz, B., Orue-Etxebaria, X., Payros, A., Bernola, G., Apellaniz, E., Caballero, F., Robador, A., Serra-Kiel, J., Tosquella, J., 2009. Redefinition of the Ilerdian stage (early Eocene). Geologica Acta 7, 177–194.
Racey, A., 1992. The relative taxonomic value of morphological characters in the genus *Nummulites* (Foraminiferida). Journal of Micropalaeontology 11, 197–209.
Raymo, M.E., Ruddiman, W.F., 1992. Tectonic forcing of late Cenozoic climate. Nature 359, 117–122.
Rodríguez-Pinto, A., Pueyo, E., Barnolas, A., Pocovi, A., Samso, J.M., Gil-Peña, I., 2006. Magnetoestratigrafia Cuisiense–Luteciense preliminar de la cuenca surpirenaica occidental. Resúmenes de MAGIBER IV — Paleomagnetismo en España y Portugal (Vigo).
Rowley, D.B., Markwick, P.J., 1992. Haq et al. Eustatic sealevel water volumes. The Journal of Geology 100, 703–715.
Samsó, J.M., Serra-Kiel, J., Tosquella, J., Travé, A., 1994. Cronoestratigrafía de las plataformas lutecienses de la zona central de la cuenca surpirenaica. In: Muñoz, A., Gonzales, A., Pérez, A. (Eds.), II Congreso Grupo Español del Terciaro, Communicaciones, Jaca, pp. 205–208.
Schaub, H., 1981. Nummulites et Assilines de la Téthys Paléogène. Taxinomie, phylogenèse et biostratigraphie. Mémoires suisses de Paléontologie 104, 105, 106, 236 p.
Schulz, M., Schäfer-Neth, C., 1997. Translating Milankovitch climate forcing into eustatic fluctuations via thermal deep water expansion: a conceptual link. Terra Nova 9, 228–231.
Séguret, M., 1972. Etude tectonique des nappes et séries décollées de la partie centrale du versant sud des Pyrénées. Caractère synsédimentaire, rôle de la compression et de la gravité. : Série Géol. Struct., 2. Publ. Univ. Sci. Tech. Languedoc, Montpellier, France. (155 pp.).
Séranne, M., 1999. Early Oligocene stratigraphic turnover on West Africa continental margin: a signature of the Tertiary greenhouse to icehouse transition? Terra Nova 11, 135–140.
Serra-Kiel, J., Hottinger, L., Caus, E., Drobne, K., Ferrández, C., Jauhri, A.K., Les, G., Pavlovec, R., Pignatti, J., Samsó, J.M., Schaub, H., Sirel, E., Strougo, A., Tambareau, Y., Tosquella, J., Zabrevskaya, E., 1998. Larger foraminiferal biostratigraphy of the Tethyan Paleocene and Eocene. Bulletin de la Société Géologique de France 169, 281–299.
Serra-Kiel, J., Mato, E., Saula, E., Travé, A., Ferràndez-Cañadell, C., Busquets, P., Samso, J.-M., Tosquella, J., Barnolas, A., Alvarez-Pérez, G., Franquès, J., Romero, J., 2003. An inventory of the marine and transitional Middle/Upper Eocene deposits of the Southeastern Pyrenean Foreland basin (NE Spain). Geologica Acta 1, 201–229.
Sinclair, H.D., 1997. Tectonostratigraphic model for underfilled peripheral foreland basins; an Alpine perspective. Geological Society of America Bulletin 109, 324–346.
Sinclair, H., Sayer, Z.R., Tucker, M.E., 1998. Carbonate sedimentation during early foreland basin subsidence: the Eocene succession of the French Alps. In: Wright, V.P., Burchette, T.P. (Eds.), Carbonate Ramps: Geological Society of London Special Publication, 149, pp. 205–227.
Sztràkos, K., Castelltort, S., 2001. La sédimentologie et les foraminifères bartoniens et priaboniens des coupes d'Arguis (Prépyrénées aragonaises, Espagne). Incidence sur la corrélation des biozones à la limite Bartonien/Priabonien. Revue de Micropaléontologie 44, 233–247.
Travé, A., Serra-Kiel, J., Zamarreno, I., 1996. Paleoecological interpretation of transitional environments in Eocene carbonates (NE Spain). Palaios 11, 141–160.
Tripati, A., Backman, J., Elderfield, H., Ferretti, P., 2005. Eocene bipolar glaciation associated with global carbon cycle changes. Nature 436, 341–346.
Vera, J., 2004. Geologia de España, Sociedad Geologica de España. Instituto Geologico y Minero de España. . (890 p.).
Vergés, J., Muñoz, J.A., 1990. Thrust sequences in the southern central Pyrenees. Bulletin de la Société Géologique de France 8, 265–271.
Vergés, J., Millán, H., Roca, E., Muñoz, J.A., Cirés, J., den Bezemer, T., Zoetemeijer, R., Cloetingh, S., 1995. Eastern Pyrenees and related foreland basins: pre-, syn- and post-collisional crustal-scale cross-section. Marine and Petroleum Geology 12, 903–915.
Vergés, J., Marzo, M., Santaeulària, T., Serra-Kiel, J., Burbank, D.W., Muñoz, J.A., Giménez-Montsant, J., 1998. Quantified vertical motions and tectonic evolution of the SE Pyrenean foreland basin. Geological Society of London Special Publications 134, 107–134.
Vergés, J., Marzo, M., Muñoz, J.A., 2002. Growth strata in foreland settings. Sedimentary Geology 146, 1–9.
Villa, G., Fioroni, C., Pea, L., Bohaty, S., Persico, D., 2008. Middle Eocene–late Oligocene climate variability: calcareous nannofossil response at Kerguelen Plateau, Site 748. Marine Micropaleontology 69, 173–192.
Vincent, S., 2001. The Sis palaeovalley: a record of proximal fluvial sedimentation and drainage basin development in response to Pyrenean mountain building. Sedimentology 48, 1235–1278.
Walker, R.G., Plint, A.G., 1992. Wave- and storm-dominated shallow marine systems. In: Walker, R.G., James, N.P. (Eds.), Facies Models—Response to Sea-level Changes. : Geological Association of Canada. St. John's, Newfoundland, Canada, pp. 219–238.
Zachos, J.C., Pagani, M., Sloan, L., Thomas, E., Billups, K., 2001. Trends, rhythm, and aberrations in global climate 65 Ma to present. Science 292, 686–693.
Zachos, J.C., Dickens, G.R., Zeebe, R.E., 2008. An early Cenozoic perspective on greenhouse warming and carbon-cycle dynamics. Nature 451, 279–283.